ENVIRONMENTAL STUDIES

Earth beyond six of nine planetary boundaries

Katherine Richardson[1]*, Will Steffen[2]†, Wolfgang Lucht[3,4], Jørgen Bendtsen[1], Sarah E. Cornell[5], Jonathan F. Donges[3,5], Markus Drüke[3], Ingo Fetzer[5,6], Govindasamy Bala[7], Werner von Bloh[3], Georg Feulner[3], Stephanie Fiedler[8], Dieter Gerten[3,4], Tom Gleeson[9,10], Matthias Hofmann[3], Willem Huiskamp[3], Matti Kummu[11], Chinchu Mohan[8,12,13], David Nogués-Bravo[1], Stefan Petri[3], Miina Porkka[11], Stefan Rahmstorf[3,14], Sibyll Schaphoff[3], Kirsten Thonicke[3], Arne Tobian[3,5], Vili Virkki[11], Lan Wang-Erlandsson[3,5,6], Lisa Weber[8], Johan Rockström[3,5,15]

This planetary boundaries framework update finds that six of the nine boundaries are transgressed, suggesting that Earth is now well outside of the safe operating space for humanity. Ocean acidification is close to being breached, while aerosol loading regionally exceeds the boundary. Stratospheric ozone levels have slightly recovered. The transgression level has increased for all boundaries earlier identified as overstepped. As primary production drives Earth system biosphere functions, human appropriation of net primary production is proposed as a control variable for functional biosphere integrity. This boundary is also transgressed. Earth system modeling of different levels of the transgression of the climate and land system change boundaries illustrates that these anthropogenic impacts on Earth system must be considered in a systemic context.

INTRODUCTION

The planetary boundaries framework (*1*, *2*) draws upon Earth system science (*3*). It identifies nine processes that are critical for maintaining the stability and resilience of Earth system as a whole. All are presently heavily perturbed by human activities. The framework aims to delineate and quantify levels of anthropogenic perturbation that, if respected, would allow Earth to remain in a "Holocene-like" interglacial state. In such a state, global environmental functions and life-support systems remain similar to those experienced over the past ~10,000 years rather than changing into a state without analog in human history. This Holocene period, which began with the end of the last ice age and during which agriculture and modern civilizations evolved, was characterized by relatively stable and warm planetary conditions. Human activities have now brought Earth outside of the Holocene's window of environmental variability, giving rise to the proposed Anthropocene epoch (*4*, *5*).

Planetary-scale environmental forcing by humans continues and individual Earth system components are, to an increasing extent, in disequilibrium in relation to the changing conditions. As a consequence, the post-Holocene Earth is still evolving, and ultimate global environmental conditions remain uncertain. Paleoclimate research, however, documents that Earth has previously experienced largely ice-free conditions during warm periods (*6*, *7*) with correspondingly different states of the biosphere. It is clearly in humanity's interest to avoid perturbing Earth system to a degree that risks changing global environmental conditions so markedly. Ice cover is only one indicator of substantial system-wide change in numerous other Earth system dimensions. The planetary boundaries framework delineates the biophysical and biochemical systems and processes known to regulate the state of the planet within ranges that are historically known and scientifically likely to maintain Earth system stability and life-support systems conducive to the human welfare and societal development experienced during the Holocene.

Currently, anthropogenic perturbations of the global environment are primarily addressed as if they were separate issues, e.g., climate change, biodiversity loss, or pollution. This approach, however, ignores these perturbations' nonlinear interactions and resulting aggregate effects on the overall state of Earth system. Planetary boundaries bring a scientific understanding of anthropogenic global environmental impacts into a framework that calls for considering the state of Earth system as a whole.

For >3 billion years, interactions between the geosphere (energy flow and nonliving materials in Earth and atmosphere) and biosphere (all living organisms/ecosystems) have controlled global environmental conditions. Earth system's state changed in response to forcings generated by external perturbations (e.g., solar energy input and bolide strikes) or internal processes in the geosphere (e.g., plate tectonics and volcanism) or biosphere (e.g., evolution of photosynthesis and rise of vascular plants). These forcings were processed through interactions and feedbacks among processes and systems within Earth system, shaping its often complex overall response. Today, human activities with planetary-scale effects act as additional forcing on Earth system. Thus, the anthroposphere has become an additional functional component of Earth system (*3*, *8*), capable of altering Earth system state. The planetary boundaries framework formulates limits to the impact of the anthroposphere on Earth system by identifying a scientifically based safe operating

[1]Globe Institute, Faculty of Health, University of Copenhagen, Copenhagen, Denmark. [2]Australian National University, Canberra, Australia. [3]Potsdam Institute for Climate Impact Research (PIK), Member of the Leibniz Association, Potsdam, Germany. [4]Department of Geography, Humboldt-Universität zu Berlin, Berlin, Germany. [5]Stockholm Resilience Centre, Stockholm University, Stockholm, Sweden. [6]Bolin Centre for Climate Research, Stockholm University, Stockholm, Sweden. [7]Centre for Atmospheric and Oceanic Sciences, Indian Institute of Science, Bangalore, Karnataka – 560012, India. [8]GEOMAR Helmholtz Centre for Ocean Research Kiel and Faculty for Mathematics and Natural Sciences, Christian-Albrechts-University Kiel, Kiel, Germany. [9]Department of Civil Engineering, University of Victoria, Victoria, British Columbia, Canada. [10]School of Earth and Ocean Sciences, University of Victoria, Victoria, British Columbia, Canada. [11]Water and Development Research Group, Aalto University, Espoo, Finland. [12]Global Institute for Water Security, University of Saskatchewan, Saskatoon, Saskatchewan, Canada. [13]Waterplan (YC S21), San Francisco, CA, USA. [14]Institute of Physics and Astronomy, University of Potsdam, Potsdam, Germany. [15]Institute for Environmental Science and Geography, University of Potsdam, Potsdam, Germany.
*Corresponding author. Email: kari@sund.ku.dk
†Deceased.

space for humanity that can safeguard both Earth's interglacial state and its resilience.

The Holocene state of Earth is the benchmark reference in this context, as many of the components comprising the planetary boundary framework were rather stable during this period. This is also the only Earth system state civilizations have historically known. Climate is a manifestation of external forcing, e.g., solar activity, orbital cycles, and interactions among Earth system components, and global mean surface temperature varied by only ±0.5°C (*9*) from the Neolithic [~9000 before the present (B.P.)] until the Industrial Revolution. Biomes across Earth have also largely been stable over the past 10,000 years, with preindustrial global terrestrial net primary production (NPP) varying by not >55.9 ± 1.1 billion tonnes (Gt) of C $year^{-1}$ (2σ) (see the Supplementary Materials). Bias-corrected data (*10*) confirm that preindustrial global precipitation levels were also stable, particularly from the mid-Holocene onward. These data provide strong support for using the Holocene (see the Supplementary Materials) as the planetary boundaries reference state for a stable and resilient planet.

All of the framework's individual boundaries therefore adopt preindustrial Holocene conditions as a reference for assessing the magnitude of anthropogenic deviations. Available data and state of knowledge from analytics and modeling of the framework components dictate the methods for derivation and quantification of the individual boundaries and their precautionary guardrails. Despite data constraints, efforts have been made to identify suitable control variables for all boundaries, together with evidence of how much perturbation leads to generation of impacts or altered interactions/feedbacks that can potentially cause irreversible changes to Earth's life support systems. The focus is always at Earth system rather than regional scale, even when the evidence used to establish boundaries originates from regional studies. In these cases, regional evidence is combined to assess Earth system impacts of cumulative transgressions across multiple regional systems.

The planetary boundaries framework has attracted considerable scientific and societal attention, inspiring governance strategies and policies at all levels. The framework evolves through updates made in light of recent scientific understanding. Here, we bring together advances from different fields of science to update the framework and the status of its boundaries. Boundaries are, for the first time, proposed for all of the individual components of the framework. Updates of the functional biosphere integrity and aerosol loading boundaries are based on analyses presented here. Recent analyses form the basis for updates of the freshwater change and novel entities boundaries. Last, the importance of considering human impacts on components of the global environment in a system context is illustrated using a modeling exercise exploring how various scenarios of transgression of the land system (representing the biosphere) and climate change boundaries combine to affect Earth system characteristics.

Framework components

Understanding how biosphere, anthroposphere, and geosphere processes interact with one another is a prerequisite for developing reliable projections of possible future Earth system trajectories. A fully process-based understanding of the interactions between these domains is, however, still only partially available. The planetary boundaries framework calls for more deeply integrated modeling of Earth system by bringing together currently available evidence for the relevant processes and their interactions from different disciplines and sources.

The nine boundaries all represent components of Earth system critically affected by anthropogenic activities and relevant to Earth's overall state. For each of the boundaries, control variables are chosen to capture the most important anthropogenic influence at the planetary level of the boundary in focus. For example, land system change arises from myriad human activities, ultimately aggregating to alteration of biomes. From a planetary perspective however, during the Holocene, forests were the land biome with the strongest functional coupling to the climate system (*11*, *12*). Therefore, global reduction in forest area is adopted as the control variable representing all land system change. Similarly, the control variable introduced here for the functional component of the biosphere integrity boundary, human appropriation of NPP (HANPP), focuses on the ability of the biosphere as a whole to provide functional feedbacks in Earth system. Control variables should ideally lend themselves to empirical determination and be computable for use in Earth system projections (e.g., process-based simulation of future change in forest cover) where possible.

Boundary positions do not demarcate or predict singular threshold shifts in Earth system state. They are placed at a level where the available evidence suggests that further perturbation of the individual process could potentially lead to systemic planetary change by altering and fundamentally reshaping the dynamics and spatiotemporal patterns of geosphere-biosphere interactions and their feedbacks (*13*, *14*).

Zone of increasing risk (of Earth system losing Holocene-like characteristics) is now used to assess the status for transgressed boundaries rather than the "zone of uncertainty" (*2*) as demarcation of this zone is based on more than what is usually referred to as scientific uncertainty. A large body of recent research [e.g., (*15*–*17*)] provides strong evidence supporting the conclusion (*2*) that the climate change and biosphere integrity boundaries are in a zone of rapidly increasing and systemically linked risks. This strengthens the rationale for using the precautionary principle to set the planetary boundaries at the lower end of the zone of increasing risk. For example, for the climate change planetary boundary, we retain the boundary of 350 parts per million (ppm) CO_2 with the zone of increasing risk ranging from 350 to 450 ppm before reaching high risk. This corresponds approximately to a range of global mean surface temperature rise of 1° to 2°C (assuming mainstream scenarios on non-CO_2 forcing). Precaution places the planetary boundary at the start of increasing risk (350 ppm ≈ 1°C), i.e., slightly below the 1.5°C target identified in the Paris Agreement. The 1.5°C target is one that science increasingly demonstrates is associated with substantial risk of triggering irreversible large change and that crossing tipping points cannot be excluded even at lower temperature increases (*18*). In recognition of the buffering resilience of Earth system, most boundaries are nevertheless set at values higher than their observed range through the Holocene up to the Industrial Revolution (for CO_2 ≈ 280 ppm) (see the Supplementary Materials). The stability and characteristic range of variability of interglacial Earth system states in Pleistocene paleoclimate (*19*) and Earth system modeling (*20*) suggest that Earth system would likely remain in a stable, Holocene-like state if all boundaries were respected despite their being at least temporarily outside the envelope of Holocene variability.

The distinction between zones of "increasing" and "high" risk cannot be sharply defined. There is accumulating evidence that the current level of boundary transgression has already taken Earth system beyond a "safe" zone. However, we still lack a comprehensive, integrated theory, backed by observations and modeling studies, that can identify when a transition from a rising level of risk to one with very high and dangerous risks of losing a Holocene-like Earth system state may occur. Therefore, the "burning embers" approach introduced by the Intergovernmental Panel on Climate Change (IPCC) to represent the gradual transitions from moderate (yellow) to high (red) to very high (purple) risks is adopted here.

Throughout Earth's history, geosphere-biosphere interactions were an internal driver of Earth system state. The climate change planetary boundary is used here as a proxy for the geosphere. Therefore, climate change and biosphere integrity are identified as "core boundaries" (*2*) in the framework. The introduction of novel entities is a new anthropogenic driver of Earth system change that, if sufficiently transgressed, could, on its own, alter Earth system state. However, this planetary boundary acts largely through perturbation of the core boundaries, especially biosphere integrity. In contrast to the definition applied earlier (*2*) where "naturally occurring elements mobilized by anthropogenic activities" were included, the definition of novel entities is now restricted to include only entities that, in the absence of the anthroposphere, are not present in Earth system.

Quantifying interactions between boundaries remains a major challenge. However, some progress has been made since the last framework update (*2*). Recent studies (*13*, *14*, *21*, *22*) have shown that additional or more extensive transgression of one planetary boundary can change risk gradients for other boundaries. For example, there is increasing evidence to suggest that transgressing either the climate change or biosphere integrity planetary boundary can potentially lead to more steeply increasing risk in the other (*21*). In the current absence of a comprehensive Earth system model that fully captures interactions between all component spheres, we explore below how various scenarios of transgression of the land system (representing the biosphere) and climate change boundaries combine to control biologically mediated carbon storage at the planetary level.

RESULTS

Biosphere integrity

Myriad interactions with the geosphere make the biosphere a constitutional component of Earth system and a major factor in regulating its state. The planetary functioning of the biosphere ultimately rests on its genetic diversity, inherited from natural selection not only during its dynamic history of coevolution with the geosphere but also on its functional role in regulating the state of Earth system. Genetic diversity and planetary function, each measured through suitable proxies, are therefore the two dimensions that form the basis of a planetary boundary for biosphere integrity. As applied here, "integrity" does not imply an absence of biosphere change but, rather, change that preserves the overall dynamic and adaptive character of the biosphere.

Rockström *et al.* (*1*) defined the planetary boundary for change in genetic diversity as the maximum extinction rate compatible with preserving the genetic basis of the biosphere's ecological complexity. We retain the boundary level of <10 E/MSY (extinctions per million species-years). The extinction rate control variable is challenging to apply in operational contexts, but data and methods for directly assessing the genetic diversity component of biosphere integrity are emerging [(*23*) and the Supplementary Materials]. Although the baseline rate of extinctions (and of new species' evolution) is both highly variable and difficult to quantify with confidence through geological time, the current rate of species extinctions is estimated to be at least tens to hundreds of times higher than the average rate over the past 10 million years and is accelerating (*24*). We conservatively set the current value for the extinction rate at >100 E/MSY (*24*–*26*). Of an estimated 8 million plant and animal species, around 1 million are threatened with extinction (*16*), and over 10% of genetic diversity of plants and animals may have been lost over the past 150 years (*23*). Thus, the genetic component of the biosphere integrity boundary is markedly exceeded (Fig. 1 and Table 1).

Previously, Steffen *et al.* (*2*) proposed using the Biodiversity Intactness Index (BII) (*27*), an empirically based metric of human impacts on population abundances, as an interim proxy for functional biosphere integrity. It was noted, however, that the link of BII to Earth system functions remains poorly understood and BII cannot be directly linked to the planetary biogeochemical and energy flows relevant for establishing Earth system state. In addition, BII relies on expert elicitation to estimate temporal changes in species abundances/distributions, and this knowledge is not readily available for many regions, including the oceans. Martin *et al.* (*28*) have also recently suggested that BII only partially reflects human impacts on Earth system.

We therefore now replace this metric with a computable proxy for photosynthetic energy and materials flow into the biosphere (*29*), i.e., net primary production (NPP), and define the functional component of the biosphere integrity boundary as a limit to the human appropriation of the biosphere's NPP (HANPP) as a fraction of its Holocene NPP. NPP is fundamental for both ecosystems and human societies as it supports their maintenance, reproduction, differentiation, networking, and growth. Biomes depend on the energy flow associated with NPP to maintain their planetary ecological functions as integral parts of Earth system. NPP-based energy flows into human societies should therefore not substantially compromise the energy flow to the biosphere (*30*). The proxy complements the diversity-based dimensions of biosphere integrity, covered by the genetic component, which captures the importance of variability in living organisms for the functioning of ecosystems. The suitability of NPP and HANPP for defining a planetary boundary has previously been discussed by Running (*31*) and Haberl *et al.* (*32*).

We determine the terrestrial biosphere's Holocene NPP to have been 55.9 Gt of C year^{-1} (2σ) and exceedingly stable, varying by not more than ±1.1 Gt of C year^{-1} despite regional variations in time (see the Supplementary Materials). Our model analyses suggest that NPP still had a Holocene-like level in 1700 (56.2 Gt of C year^{-1} for potential natural vegetation and 54.7 Gt of C year^{-1} when land use is taken into account). By 2020, potential natural NPP would have risen to 71.4 Gt of C year^{-1} because of carbon fertilization, a disequilibrium response of terrestrial plant physiology to anthropogenically increasing CO_2 concentration in the atmosphere, whereas actual NPP was 65.8 Gt of C year^{-1} due to the

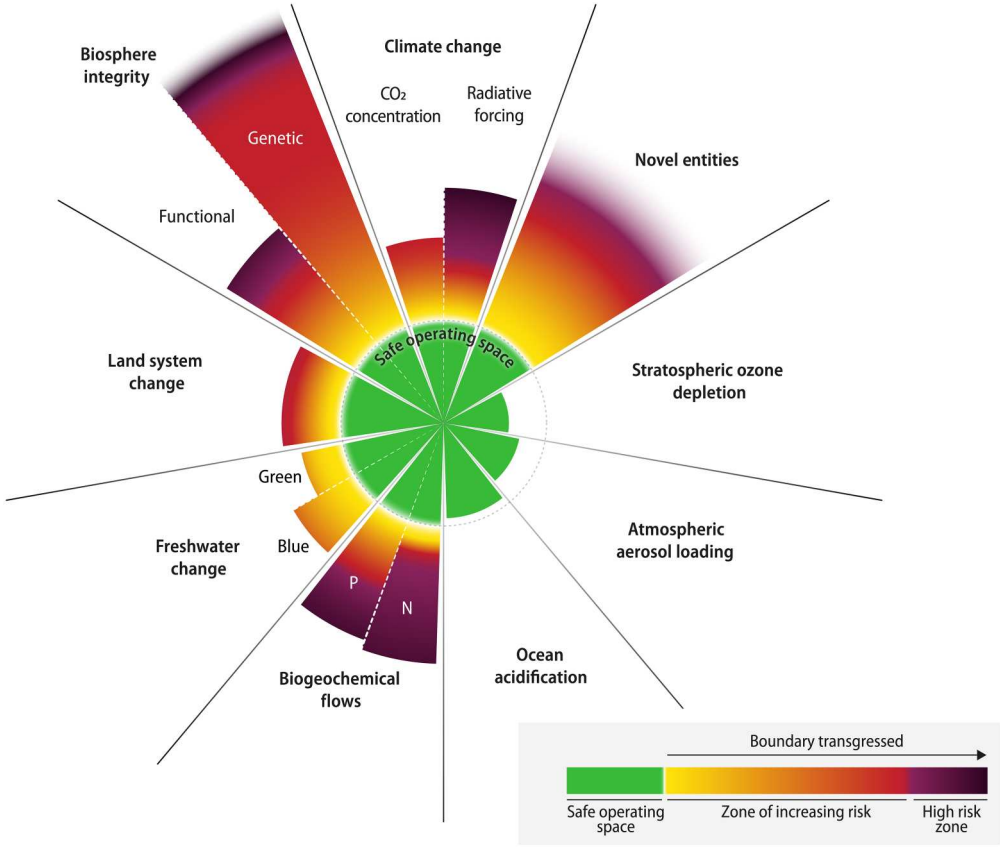

Fig. 1. Current status of control variables for all nine planetary boundaries. Six of the nine boundaries are transgressed. In addition, ocean acidification is approaching its planetary boundary. The green zone is the safe operating space (below the boundary). Yellow to red represents the zone of increasing risk. Purple indicates the high-risk zone where interglacial Earth system conditions are transgressed with high confidence. Values for control variables are normalized so that the origin represents mean Holocene conditions and the planetary boundary (lower end of zone of increasing risk, dotted circle) lies at the same radius for all boundaries (except for the wedges representing green and blue water, see main text). Wedge lengths are scaled logarithmically. The upper edges of the wedges for the novel entities and the genetic diversity component of the biosphere integrity boundaries are blurred either because the upper end of the zone of increasing risk has not yet been quantitatively defined (novel entities) or because the current value is known only with great uncertainty (loss of genetic diversity). Both, however, are well outside of the safe operating space. Transgression of these boundaries reflects unprecedented human disruption of Earth system but is associated with large scientific uncertainties.

NPP-reducing effects of global land-use (see the Supplementary Materials).

HANPP designates both the harvesting and the elimination or alteration (mostly reduction) of potential natural NPP (*32*), mainly through agriculture, silviculture, and grazing. Terrestrial HANPP can be estimated both as a fraction of potential natural NPP [15.7% in 1950 and 23.5% in 2020; inferred from (*33*) and the Supplementary Materials] and of Holocene mean NPP (30% or 16.8 Gt of C $year^{-1}$ in 2020; see the Supplementary Materials). We argue that an NPP-based planetary boundary limiting HANPP should be set in relation to preindustrial Holocene mean NPP and not the current potential natural NPP. This is because the global increase in NPP due to anthropogenic carbon fertilization constitutes a resilience response of Earth system that dampens the magnitude of anthropogenic warming. Hence, the NPP contribution to a carbon sink associated with CO_2 fertilization should be protected and sustained rather than considered as being available for harvesting. Examples of large land areas under human use with declining carbon sinks, some even turning into carbon sources, i.e., due to human overexploitation of biomass, are already being observed, for example, in some Amazonian regions (*34*) and northern European forests.

As NPP is the basis for the energy and materials flow that underpins the biosphere's functioning (*30*), we argue that today's planetary-scale impact of HANPP is reflected in the observation that major indicators of the state of the biosphere show large and worrisome declines in recent decades (*16*). This suggests that current HANPP is well beyond a precautionary planetary boundary aiming to safeguard the functional integrity of the biosphere and likely already into the high-risk zone. We therefore provisionally set the functional component of the biosphere integrity planetary boundary at human appropriation of 10% of preindustrial Holocene mean NPP, shifting into the zone of high risk at 20%. The boundary thus defined was transgressed in the late 19th century, a time of considerable acceleration in land use globally (*35*) with strong impacts on species (*27*), already leading to early concerns about the effects of this large-scale land transformation.

Thus, while the climate warming problem became evident in the 1980s, problems arising in functional biosphere integrity due to human land use began a century earlier. Since the 1960s, growth

Table 1. Current status for the planetary boundaries.

Earth system process	Control variable(s)	Planetary boundary	Preindustrial Holocene base value	Upper end of zone of increasing risk	Current value of control variable
Climate change	Atmospheric CO_2 concentration (ppm CO_2)	350 ppm CO_2	280 ppm CO_2	450 ppm CO_2	417 ppm CO_2 (*41*)
	Total anthropogenic radiative forcing at top-of-atmosphere (W m^{-2})	+1.0 W m^{-2}	0 W m^{-2}	+1.5 W m^{-2}	+2.91 W m^{-2} (*41*)
Change in biosphere integrity	Genetic diversity: E/MSY	<10 E/MSY but with an aspirational goal of ca. 1 E/MSY (assumed background rate of extinction loss)	1 E/MSY	100 E/MSY	>100 E/MSY (*24–26*)
	Functional integrity: measured as energy available to ecosystems (NPP) (% HANPP)	HANPP (in billion tonnes of C $year^{-1}$) <10% of preindustrial Holocene NPP, i.e., >90% remaining for supporting biosphere function	1.9% (2σ variability of preindustrial Holocene century-mean NPP)	20% HANPP	30% HANPP (see the Supplementary Materials)
Stratospheric ozone depletion	Stratospheric O_3 concentration, (global average) (DU)	<5% reduction from preindustrial level assessed by latitude (~276 DU)	290 DU	261 DU	284.6 DU (*96*)
Ocean acidification	Carbonate ion concentration, average global surface ocean saturation state with respect to aragonite (Ω_{arag})	≥80% Ω_{arag} of mean preindustrial aragonite saturation state of surface ocean, including natural diel and seasonal variability	3.44 Ω_{arag}	2.75 Ω_{arag}	2.8 Ω_{arag} (*71*)
Biogeochemical flows: P and N cycles	Phosphate *global:* P flow from freshwater systems into the ocean; *regional*: P flow from fertilizers to erodible soils (Tg of P $year^{-1}$)	Phosphate *global:* 11 Tg of P $year^{-1}$; *regional:* 6.2 Tg of P $year^{-1}$ mined and applied to erodible (agricultural) soils. Boundary is a global average, but regional distribution is critical for impacts.	0 Tg of P $year^{-1}$	*Global*: 100 Tg of P $year^{-1}$; *regional*: 11.2 Tg of P $year^{-1}$	*Global*: 22.6 Tg of P $year^{-1}$ (*75*); *regional*: 17.5 Tg of P $year^{-1}$ (*76*)
	Nitrogen *global:* industrial and intentional fixation of N (Tg of N $year^{-1}$)	Nitrogen *global:* 62 Tg of N $year^{-1}$. Boundary is a global average. Anthropogenic biological N fixation on agriculture areas highly uncertain but estimates in range of ~30 to 70 Tg of N $year^{-1}$. Boundary acts as a global "valve" limiting introduction of new reactive N to Earth system, but regional distribution of fertilizer N is critical for impacts.	0 Tg of N $year^{-1}$	82 Tg of N $year^{-1}$	190 Tg of N $year^{-1}$ (*84*)
Land system change	*Global*: area of forested land as the percentage of original forest cover; *biome*: area of forested land as the percentage of potential forest (% area remaining)	*Global: 75%* values are a weighted average of the three individual biome boundaries; *biomes*: tropical, 85%; temperate, 50%; boreal: 85%	100%	*Global:* 54%; *biomes*: tropical, 60%; temperate, 30%; boreal: 60%	*Global*: 60% [(*72*, *97*) and see the Supplementary Materials]; *tropical*: Americas, 83.9%; Africa, 54.3%; Asia, 37.5%; *temperate*: Americas, 51.2%; Europe, 34.2%; Asia, 37.9%; *boreal*: Americas, 56.6%; Eurasia: 70.3%
Freshwater change	Blue water: human induced disturbance of blue water flow	Upper limit (95th percentile) of global land area with deviations greater than during preindustrial, Blue water: 10.2%	9.4% (median of preindustrial conditions)	50% (provisional)	18.2% (*46*)
	Green water: human induced disturbance of	Green water: 11.1%		50% (provisional)	15.8% (*46*)

continued on next page

Earth system process	Control variable(s)	Planetary boundary	Preindustrial Holocene base value	Upper end of zone of increasing risk	Current value of control variable
	water available to plants (% land area with deviations from preindustrial variability)		9.8% (median of preindustrial conditions)		
Atmospheric aerosol loading	Interhemispheric difference in AOD	0.1 (mean annual interhemispheric difference)	0.03	0.25	0.076 (*55*, *57*, *68*)
Novel entities	Percentage of synthetic chemicals released to the environment without adequate safety testing	0	0	NA	Transgressed

in global population and consumption further accelerated land use, driving the system further into the zone of increasing risk. HANPP has always sustained humanity's need for food, fiber, and fodder, and this will continue to be the case in the future, as well as for sustainable societies. The NPP required to support future societies must, however, increasingly be generated through additional production of NPP above the Holocene baseline, not including the NPP generated for biology-based carbon sinks. Feeding 10 billion people, for example, is theoretically possible within planetary boundaries but requires a number of far-reaching transformations to improve the impacts of production and regulate demand (*36*).

To develop a deeper foundation for the HANPP-based planetary boundary for functional biosphere integrity, we need an improved understanding of how ecological dynamics generate the functions of the biosphere in Earth system. Analysis of NPP should be spatially explicit and augmented by computable metrics of ecological destabilization due to climate and land use pressures, e.g., a metric of biogeochemical disruption (*37*).

HANPP can also be quantified for marine systems. About two-thirds of the ocean area where HANPP is >10% is found above the shallow shelf areas (*38*) where ecosystems are most intensely exploited. Regionally, fish catches exceed thresholds of sustainable exploitation (*39*). However, in contrast to land, where most HANPP occurs in the form of plant material, i.e., at the lowest trophic level, HANPP in the ocean tends to take place at higher trophic levels. This means that while HANPP reduces the absolute amount of energy available to higher trophic levels on land, much of the energy fixed through NPP is used in marine ecosystems before HANPP occurs. When the abundance of organisms at the highest trophic levels is reduced, changes in marine ecosystem structure may change energy flow in these ecosystems (*40*). Thus, in the marine realm, HANPP likely changes the flows rather than the amount of energy available. More information about the impacts of HANPP in the marine realm is necessary to integrate consideration of the marine systems in the functional biosphere integrity planetary boundary.

Climate change

Climate change control variables and boundary levels are retained (*1*, *2*). The most important drivers of anthropogenic impacts on Earth's energy budget are the emission of greenhouse gases and aerosols, and surface albedo changes (*17*). The control variables in the framework are the annual averages of atmospheric CO_2 concentration and the change in radiative forcing. The planetary boundary for atmospheric CO_2 concentration is set at 350 ppm and for radiative forcing at 1 W m^{-2}. Currently, the estimated total anthropogenic effective radiative forcing is 2.91 W m^{-2} [2022 estimate, relative to 1750 (*17*)], and atmospheric CO_2 concentration is 417 ppm [annual mean marine surface value for 2022 (*41*)], i.e., further outside the safe operating space on both measures than in the last update (*2*). The 350-ppm boundary would lead to a lower level of anthropogenic global warming than the internationally agreed 1.5°C target in the United Nations Paris Climate Agreement but is consistent with recent studies (*17*, *18*, *42*) suggesting the possibility of extreme Earth system impacts even at 1.5° warming, with risks increasing already markedly above 1° warming.

Novel entities

The definition of this boundary is now restricted to truly novel anthropogenic introductions to Earth system. These include synthetic chemicals and substances (e.g., microplastics, endocrine disruptors, and organic pollutants); anthropogenically mobilized radioactive materials, including nuclear waste and nuclear weapons; and human modification of evolution, genetically modified organisms and other direct human interventions in evolutionary processes. Novel entities serve as geological markers of the Anthropocene (*5*). However, their impacts on Earth system as a whole remain largely unstudied. The planetary boundaries framework is only concerned with the stability and resilience of Earth system, i.e., not human or ecosystem health. Thus, it remains a scientific challenge to assess how much loading of novel entities Earth system tolerates before irreversibly shifting into a potentially less habitable state.

Hundreds of thousands of synthetic chemicals are now produced and released to the environment. For many substances, the potentially large and persistent effects on Earth system processes of their introduction, particularly on functional biosphere integrity, are not well known, and their use is not well regulated. Humanity has repeatedly been surprised by unintended consequences of this release, e.g., with respect to the release of insecticides such as DDT and the effect of chlorofluorocarbons (CFCs) on the ozone layer. For this class of novel entities, then, the only truly safe operating space that can ensure maintained Holocene-like conditions is one where these entities are absent unless their potential impacts with respect to Earth system have been thoroughly evaluated. This would imply that the quantified planetary boundary should be set at zero release of synthetic chemical compounds to the open environment

unless they have been certified as harmless and are monitored. That is the target set by the Montreal Protocol with respect to the substances shown to be harmful by contributing to depletion of the ozone layer.

In their analysis of various strategies for establishing a planetary boundary for novel entities, Persson *et al.* (*43*) identified the share of released chemicals with adequate safety assessment and monitoring as a candidate control variable. We here adopt this metric. The planetary boundary is then set at the release into Earth system of 0% of untested synthetics. When synthetics released to the environment are thoroughly tested, the ensuing risk of damaging effects is lowered. Admittedly, this approach has weaknesses: Data availability is incomplete; safety studies often focus on narrowly defined toxicity and do not capture the "cocktail effects" of chemical mixtures in the environment nor their effects under specific conditions. The percentage of untested synthetics released globally is unknown. However, Persson *et al.* (*43*) report that for the chemicals currently registered under the EU Registration, Evaluation, Authorisation and Restriction of Chemicals (REACH) regulation (a small subset of the chemical universe), ~80% of these chemicals had been in use for at least 10 years without yet having undergone a safety assessment. Likewise, few safety studies consider potential Earth system effects. With such an enormous percentage of untested chemicals being released to the environment, a novel entities boundary defined in this manner is clearly breached. Persson *et al.* (*43*) did not identify or quantify a singular planetary boundary for novel entities but, nevertheless, also concluded that the safe operating space is currently overstepped.

Stratospheric ozone depletion

Stratospheric ozone depletion is a special case related to the anthropogenic release of novel entities where gaseous halocarbon compounds from industry and other human activities released into the atmosphere lead to long-lasting depletion of Earth's ozone layer. The boundary for the safe operating space is set at 276 Dobson units (DU), i.e., allowing a <5% reduction from the preindustrial level of 290 DU, assessed by latitude (*1*). Following the ratification of the Montreal Protocol in 1987, the trend and global extent of ozone depletion have recovered slightly (*44*, *45*). The current (2020) global estimate is 284 DU (see the Supplementary Materials). Thus, the human perturbation of the stratospheric ozone depletion has decreased and is now within the safe operating space. The boundary for ozone depletion is currently only transgressed over the Antarctic and southern high latitudes and only in the 3-month Austral spring (*45*).

Freshwater change

To comprehensively reflect anthropogenic modifications of Earth system functions of freshwater, this boundary is revised to consider changes across the entire water cycle over land (*46*–*48*). We here use streamflow as a proxy to represent blue water (surface and groundwater) and root-zone soil moisture to represent green water (plant-available water) (*46*–*48*). Control variables are defined as the percentage of annual global ice-free land area with streamflow/root-zone soil moisture deviations from preindustrial variability (*46*, *48*). The new green water component directly accounts for hydrological regulation of terrestrial ecosystems, climate, and biogeochemical processes (*48*), whereas the blue water component accounts for river regulation and aquatic ecosystem integrity (*46*). Moreover, this boundary now captures Earth system impacts of both water increases and decreases on a monthly scale and includes their spatial patterns (see the Supplementary Materials).

The control variables describe deviations from the preindustrial (here, 1661–1860) state, first determined at the 30 arc-min grid cell scale and further aggregated to a global annual value. For both blue and green water control variables, boundaries are set at the 95th percentile of preindustrial variability, i.e., variability of the percentage of global land area with deviations [~10% for blue and ~11% for green water; (*46*) and the Supplementary Materials]. We assume that preindustrial conditions are representative of longer-term Holocene conditions and that notable deviation from this state puts freshwater's Earth system functions at risk. Pending comprehensive assessment of impacts of different transgression levels of the blue and green water boundaries (e.g., reduced carbon sequestration capacity, climate regulation, and biodiversity loss; see the Supplementary Materials), the boundary settings are preliminary and highly precautionary. Currently, ~18% (blue water) and ~16% (green water) of the global land area experience wet or dry freshwater deviations (*46*). Thus, in contrast to the earlier planetary boundary assessments (*1*, *2*) where only blue water removal was considered, this new approach indicates substantial transgression of the freshwater change boundary. Transgressions of both the blue and green water boundaries occurred a century ago, in 1905 and 1929, respectively (*46*). Thus, with the revised definition of the control variables, fresh water would have been considered transgressed already at the time of the previous planetary boundary assessments. The previous global-scale control variable would still indicate freshwater use to remain in the safe zone, even with newer data sources than those used in (*1*, *2*). Recent estimates of global blue water consumption totals ~1700 km^3 $year^{-1}$ (*49*), i.e., far below the previous boundary set at 4000 km^3 $year^{-1}$.

Atmospheric aerosol loading

Aerosols have multiple physical, biogeochemical, and biological effects in Earth system, motivating their inclusion as a planetary boundary (see the Supplementary Materials). Anthropogenic aerosol loading has increased (*50*). Changes since the preindustrial for natural aerosols (e.g., desert dust, soot from wildfires) are difficult to assess because of model differences in the sign of trends (*51*), but observational evidence suggests a global doubling of dust deposition since 1750 (*52*). At present, the Sahara is the world's largest dust source region [e.g., (*53*)], but earlier in the Holocene, it was a vegetated landscape with many lakes and wetlands (14,500 to 5000 B.P.). Changes in monsoon rainfalls, involving vegetation-dust-climate feedbacks, are thought to have terminated the "green Sahara," leading to major displacements of human settlements across parts of Africa and Asia (*54*).

Quantification of the aerosol loading planetary boundary is hampered by their multiple natural and human-caused sources, differences in chemical composition, seasonality and atmospheric lifetimes, and the consequently very large spatial and temporal heterogeneity in distribution and climatic and ecological impacts of aerosols. Nevertheless, aerosol optical depth (AOD) provides a generic control variable for aerosol loading. AOD is an integrated measure of the overall reduction in sunlight reaching Earth's surface caused by all absorption and scattering in the vertical air column. On the basis of the evidence of the impacts of large AOD on regional precipitation over southern Asia, Steffen *et al.* (*2*) set a

provisional regional planetary boundary of AOD = 0.25 (0.25 to 0.5) on the basis that higher AOD values in monsoon regions likely lead to significantly lower rainfall, ultimately affecting biosphere integrity. The annual mean AOD in southern Asia is currently about 0.3 to 0.35 (*55*, *56*). The current value for the East China region is 0.4 (*55*). Thus, aerosol loading in these regions has likely exceeded the regionally defined boundary, but with high uncertainty. Data and assessments of aerosol impacts on climate and ecosystems are lacking to determine whether this regionally defined boundary is applicable elsewhere. Global mean AOD at present is 0.14 (*57*), with much higher levels in some regions and with very strong gradients from land to open ocean (*56*).

In addition to the direct effects of AOD on regional climate and precipitation, asymmetries in AOD between northern and southern hemispheres can affect multiple monsoon systems, as seen for the West African monsoon (*58*) and Indian monsoon (*59*, *60*). The interhemispheric difference in AOD affects regional monsoon rainfall by shifting the location of the Intertropical Convergence Zone (*61*). Large asymmetries in the temperature of northern and southern hemispheres arise from differences in natural and anthropogenic aerosol emissions, land cover, and other climate forcers (*58*, *59*, *62*, *63*). The asymmetric radiative forcing resulting from aerosol effects leads to a relative cooling of the northern hemisphere and a southward shift in tropical precipitation (*64*). The interhemispheric AOD difference and its impact on tropical precipitation and water availability are sensitive to the particle size and latitudinal and altitudinal distribution of aerosols (*65*). Studies of aerosol-climate interactions following volcanic eruptions (*66*) indicate that monsoon precipitation in the northern hemisphere is weakened when northern hemisphere AOD is higher and the interhemispheric AOD difference is greater and is enhanced when more aerosols are emitted in the southern hemisphere (smaller interhemispheric AOD difference). This understanding is broadly consistent with the decrease in tropical mean precipitation after major volcanic eruptions in observations and global climate models (*67*). The IPCC AR6 has assessed that observed decreases in global land monsoon precipitation from the 1950s to the 1980s are partly attributed to human-caused northern hemisphere aerosol emissions, thus relatively larger interhemispheric difference (*17*). In addition to volcanic aerosols, monsoon dynamics and the associated regional rainfalls also respond to changes in anthropogenic aerosols (see the Supplementary Materials).

We therefore propose the annual mean interhemispheric difference in AOD as a globally defined control variable for aerosol loading. The present-day interhemispheric difference is ~0.076 ± 0.006 (mean ± SD), based on 12 observational estimates, reaching ~0.1 in the boreal spring and summers, due to the seasonal increase in dust storms that dominate in the northern hemisphere (*55*). The preindustrial annual mean value is estimated as ~0.03, based on multimodel analyses (*68*), indicating an increase in interhemispheric AOD difference by ~0.04 in the industrial era. Present-day interhemispheric AOD difference is consistent with Coupled Model Intercomparison Project 6 (CMIP6) emission inventories that show more anthropogenic aerosols in the northern hemisphere, with future projections suggesting a decrease in the asymmetry (*69*).

We assign a planetary boundary value of 0.1 for the mean annual interhemispheric difference in AOD, with high uncertainty about the zone of increasing risks, 0.1 to 0.25. In setting this boundary, we note that the impacts of aerosol loading on tropical monsoon systems are already seen today, and the impact is not only restricted to rainfall but also affects regional climate more broadly. Aerosol-cloud interaction might exacerbate effects of AOD asymmetry. The contribution of aerosol-cloud interactions to the hemispheric asymmetry of reflected shortwave radiation is unclear. Take for instance the current range of anthropogenic aerosol effective radiative forcing for present day that has been reported to be −1.6 to −0.6 W m^{-2} in the global mean for the 16 to 84% confidence interval, with aerosol-cloud interactions as a major source for uncertainty (*51*). Other large-scale effects of aerosols, such as air quality impacts on land and marine ecosystems, are also already evident (*17*, *70*). Biogenic aerosols have not been considered, despite their role in feedbacks in Earth system. A much better systemic and quantitative understanding of the hydroclimatic, ecological, and biogeochemical effects of asymmetric aerosol forcing is needed to refine the aerosol loading boundary.

Ocean acidification

The control variable used is the carbonate ion concentration in surface seawater (specifically, Ω_{arag}, the average global surface ocean saturation state with respect to aragonite). The original boundary quantification [≥80% of the preindustrial averaged global Ω_{arag} of 3.44 (*1*)] is retained. A recent estimate sets the current Ω_{arag} at ~2.8 (*71*) (see the Supplementary Materials), approximately 81% of the preindustrial value. Thus, anthropogenic ocean acidification currently lies at the margin of the safe operating space, and the trend is worsening as anthropogenic CO_2 emission continues to rise.

Land system change

This boundary focuses on the three major forest biomes that globally play the largest role in driving biogeophysical processes (*2*), i.e. tropical, temperate, and boreal. The control variable remains the same: forest cover remaining compared to the potential area of forest in the Holocene (*2*). The boundary positions remain at 85%/50%/85% for boreal/temperate/tropical forests (cf. Table 1 and the Supplementary Materials). On the basis of 2019 land-cover classification maps derived from satellite observations (*72*), the current state of the regional biomes is similar to that in 2015 although, for most regions, the amount of deforestation has increased since 2015 (see the Supplementary Materials). Land-use conversion and fires are causing rapid change in forest area (*73*, *74*), and deforestation of the Amazon tropical forest has increased such that it has now transgressed the planetary boundary (Table 1). Changes in the methodology and technology used to estimate forest cover since 2015 may be influencing the biome-level differences reported here compared to the last update (*2*). Nevertheless, there is little doubt that the global forest area continues to decrease (*74*).

Biogeochemical flows

Biogeochemical flows reflect anthropogenic perturbation of global element cycles. Currently, the framework considers nitrogen (N) and phosphorus (P) as these two elements constitute fundamental building blocks of life, and their global cycles have been markedly altered through agriculture and industry. Anthropogenic impacts on global carbon cycling are equally fundamental but are addressed in the climate and biosphere integrity boundaries. Other elements could come into focus under this boundary as an understanding of human perturbation of element cycles advances. For both N and P, the anthropogenic release of reactive forms to land and oceans is of

interest, as altered nutrient flows and element ratios have profound effects on ecosystem composition and long-term Earth system effects. Some of today's changes will only be seen on evolutionary time scales, while others are already affecting climate and biosphere integrity.

For P, we retain the regional-level and global boundaries proposed by Steffen *et al.* (*2*). The global boundary for P is a sustained flow of 11 Tg of P year^{-1} from fresh water to the ocean, to avoid large-scale anoxia. We have not found newer studies quantifying P flows in fresh water to the sea since that used for the 2015 framework update, i.e., an estimated 22 Tg of P year^{-1} (*75*). The regional level boundary is set at a flow of 6.2 Tg of P year^{-1} from fertilizers to erodible soils, to avert widespread eutrophication of freshwater ecosystems. The current rate of application of P in fertilizers to croplands is 17.5 Tg of P year^{-1} (*76*) although P use is rising and much higher estimates of up to 32.5 Tg of P year^{-1} have been reported in other studies (*77*–*79*). Thus, both the global and regional boundaries for P are exceeded. The planetary boundary for N is the application rate of intentionally fixed N to the agricultural system of 62 Tg of N year^{-1} [unchanged from (*2*)]. Currently, the application of industrially fixed N fertilizer is 112 Tg of N year^{-1} (*80*). Quantification of anthropogenic biological N fixation in connection with agriculture is highly uncertain, but the most recent estimates are in the range of ~30 to 70 Tg of N year^{-1} (*81*–*83*). According to Food and Agriculture Organization (*84*), the total introduction of anthropogenically fixed N applied to the agricultural system is ~190 Tg year^{-1} so this boundary is also globally transgressed.

DISCUSSION

Six planetary boundaries are found currently to be transgressed (Fig. 1 and Table 1). For all of the boundaries previously identified as transgressed [climate change, biosphere integrity (genetic diversity), land system change, and biogeochemical flows (N and P)], the degree of transgression has increased since 2015. We have introduced HANPP as a control variable for the functional component of biosphere integrity and argue that this boundary is also transgressed. Drawing on the considerable recent scientific progress made in refining the safe operating space for water, control variables for both green and blue water components are now included in the freshwater change planetary boundary. The boundary is transgressed for both components. Global boundaries for aerosol loading and novel entities are proposed. The novel entities boundary is transgressed. The global aerosol loading boundary is not transgressed although regional transgressions are noted.

Earth system effects of differing scenarios of transgression of land system change and climate boundaries

To illustrate the importance of considering the multiple anthropogenic impacts on the global environment in a systemic context rather than individually, we examine how varying degrees of transgression of the climate and land system change boundaries combine to influence two codeterminants of Earth system state: temperature and terrestrial carbon storage.

For climate change, the Potsdam Earth Model (POEM) [(*85*) and the Supplementary Materials] is forced by increased atmospheric carbon dioxide levels (350, 450, and 550 ppm), and land system change is forced with land-use patterns representing different extents of tropical, temperate, and boreal forest cover (see the Supplementary Materials). As some biological processes take centuries to approach a steady state, we investigate changes in both the short (1988–2100) and the long term (2100–2770). This also enables us to examine the veracity of the placement of these planetary boundaries and their zones of increasing risk in terms of critical Earth system responses.

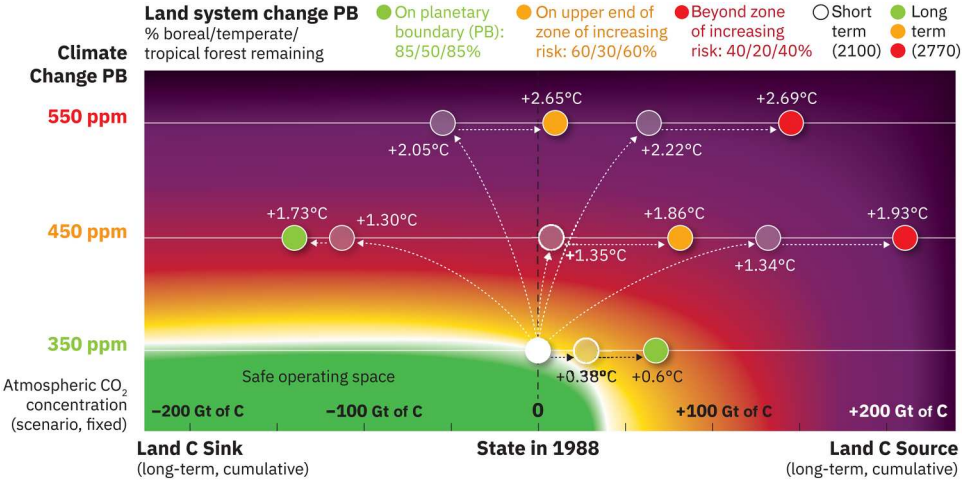

Fig. 2. Impact of the combined effect of land system change and climate change boundary states on trajectories of terrestrial carbon stocks and global land temperature. Results are based on idealized Earth system model experiments with varying planetary boundary status, ranging from maintaining the planetary boundary (85%/50%/85% boreal/temperate/tropical forest remaining, 350-ppm atmospheric CO_2, green), the upper end of the zone of increasing risk (60%/30%/60%, 450 ppm, orange), and beyond the zone of increasing risk (40%/20%/40%, 550 ppm, red). Open circles represent the short-term changes (1988–2100) of the system, while colored circles the long-term changes (2100–2770). Their colors denote the state of the land system change boundary, while the climate change boundary is shown on the *y* axis. The locations of the circles on the *x* axis represent the changes in the land carbon stocks, and the associated land temperature changes are given next to each circle, both compared to the year 1988. Transgressing the climate change boundary (*y* axis) is mostly connected to an increase in temperature, while the transgression of land system change leads to a loss of terrestrial carbon stocks (source) of 100 to 200 Gt of C.

According to these simulations, anthropogenic activities brought both climate and land system change outside of their safe operating space around 1988. Had Earth system remained forced by 1988 conditions (350 ppm and 85%/50%/85% of tropical/temperate/boreal forest cover remaining), the simulations show that temperature over the global land surface would not have increased by more than an additional 0.6°C in the subsequent 800 years (and not >1.3°C compared to the preindustrial period). Only a small (cumulative 25 Gt of C) terrestrial carbon source would have developed by 2100 and a cumulative source of not >68 Gt of C after 800 years. Thus, the exercise suggests that essentially stable planetary conditions would have been maintained had human impacts on these two boundaries remained at their 1988 levels, i.e., marginally within the safe operating space.

Both of these planetary boundaries have, however, since been transgressed into a zone of increasing risk of systemic disruption. If climate and land system change can be halted at 450 ppm and forest cover retained at 60%/30%/60% of boreal/temperate/tropical natural cover, then the simulation indicates a mean temperature rise over land of 1.4°C by 2100 (in addition to 0.7°C between preindustrial time and 1988) and 1.9°C after 800 years as vegetation evolves in a warmer climate and associated carbon fertilization (Fig. 2).

Carbon fertilization of vegetation growth counters the negative impacts of climate warming on the global average carbon sinks, leading to only moderate cumulative loss in terrestrial carbon due to additional deforestation. If, however, deforestation had been maintained at the level of the planetary boundary rather than having been allowed to rise in the zone of increasing risk, then the land biosphere would have developed a cumulative carbon sink rather than a source, contributing to stabilizing Earth's conditions. In contrast, if deforestation is allowed to breach into the high-risk zone, then simulations show a substantial additional carbon leakage to the atmosphere both over the short and long term (132 and 211 Pg of C), despite strong CO_2 fertilization of vegetation growth in the model (Fig. 2).

The situation is even more extreme if atmospheric CO_2 concentration rises above the risk zone (550 ppm; Fig. 2) and deforestation continues. Not only is the temperature on land about 2.7°C warmer than in 1988 (3.4°C warmer than preindustrial), but also around 145 Gt of C would be lost long-term from terrestrial vegetation and soils. Note that these findings reflect optimistic modeling assumptions on carbon fertilization. Many of the ecological factors not sufficiently represented in current biogeochemical models could lead to even less desirable consequences of leaving the safe operating space. These simulations illustrate clearly that human impacts on climate and forest cover must be considered in a systemic context. They furthermore support the placement of the planetary boundaries for climate and land system change at the lower end of the zone of increasing risk.

Influence of climate change on biologically mediated C sinks in the ocean

Approximately 450 Gt of C is bound up in terrestrial biota, primarily in plants (*86*), while only ~6 Gt of C is found in ocean biota (*87*). Biologically mediated marine carbon sinks are composed of particulate organic carbon (POC) that can potentially sink below the permanent thermocline (biological pump) and dissolved organic C. Via microbial breakdown of POC and dissolved organic C, CO_2 is released. When this release influences partial pressure of CO_2 in surface waters, it tends to reduce oceanic carbon uptake from the atmosphere. Microbial respiration is highly sensitive to temperature and, in a warmer ocean, an increased release of CO_2 in surface waters is predicted (*88*). The biologically mediated carbon sink in the ocean most exposed to climate change is the amount of carbon fixed by photosynthesis (NPP), i.e., POC, in the surface ocean that is ultimately transported into the ocean interior via the biological pump. When this occurs, the resulting carbon drawdown reduces partial pressure of CO_2 in the surface layer and tends to increase the atmosphere-to-ocean CO_2 flux.

These biological processes are implicitly and, in some cases, explicitly included in the CMIP6 models informing the IPCC. However, as these models configure biologically mediated carbon flows differently, there is considerable variability in their results. Models used by the IPCC do not even agree on the direction of change in NPP in response to climate change (*89*). Our model runs (see the Supplementary Materials) suggest no significant change in globally averaged ocean NPP under the different climate forcing conditions and only a modest decrease in exported material out of the surface layer [new production (ΔNP); Table 2]. Using empirical relationships (*90*, *91*) describing the transfer of carbon to the ocean interior and derived from the contemporary ocean to estimate biological pump sensitivity to future temperature increases indicates a similar weakening of the pump in the upper ocean (Table 2 and the Supplementary Materials). That these two independent methods indicate similar decreases in the export of POC from the surface layer lends confidence both in the direction and magnitude of climate impacts on this biologically mediated global carbon sink.

The analysis shows that DIC (dissolved inorganic carbon; including CO_2) accumulates over time in the ocean as a whole, particularly in the upper ocean (<1000 m; Table 2). Changes in the biologically driven accumulation rates are relatively small compared

Table 2. Global averaged change in three scenarios from the initial state (1988–2018): change in sea surface temperature (ΔSST), new production (ΔNP), and biogenic particulate flux below 500 m depth (ΔF_{500m}) including model and empirically derived values, surface saturation state of aragonite (ΔΩ), and the DIC inventory between the surface and 1000 m depth ($\Delta DIC_{0-1000m}$).

Scenario (ppm)	ΔSST (°C)	ΔNP Model (%)	ΔNP Empirical (%)	ΔF_{500m} Model (%)	ΔF_{500m} Empirical (%)	ΔΩ (—)	$\Delta DIC_{0-1000m}$ (Gt of C)
350	0.3	2.0	2.5	1.9	1.8	0.0	38
450	1.0	0.0	1.4	0.0	−3.5	−0.4	172
550	1.7	−2.5	−1.0	−3.1	−9.4	−0.7	273

to the change in the total DIC inventory that is mainly driven by the solubility pump, i.e., the tendency of increased oceanic uptake when atmospheric partial pressure of CO_2 rises. The organic matter flux below the 500-m-depth horizon (ΔF_{500m}) varies between 3 and 9% between the model and empirically derived fluxes in the 550 ppm scenario with the model-derived sensitivity being lowest. This illustrates the current uncertainty in quantifying climate-driven feedbacks on the biological pump. The implied accumulation of DIC in the surface ocean will tend to decrease the uptake of atmospheric CO_2, thus counteracting global actions for stabilizing or even reducing atmospheric CO_2 concentrations. The ocean response to reduced greenhouse gases will be complex and occur on different time scales, e.g., the characteristic response time simulated for the total carbon pool in the upper 1000 m is ~150 years (550 ppm; see the Supplementary Materials). However, the natural ocean carbon sink will gradually decrease on millennial time scales.

The reduction of sinking organic material will affect the mesopelagic ecosystem (i.e., the subsurface ecosystem between 200 and 1000 m in depth, one of the largest biomes on Earth and one that hosts numerous transient grazers, including some whales). The flux of organic material via sinking represents the energy source for organisms in this biome. A reduction of up to ~10% of energy flux would potentially have enormous consequences for this biome and, thereby, its biosphere integrity. Recent paleontological reconstructions (*92*) provide evidence that these decreases in carbon flux to the mesopelagic may have occurred in relation to past climate changes.

Acidification due to increased CO_2 reduces the saturation state of aragonite (Ω). It tends to hinder the biological formation of calcium carbonate, an essential component for shell and reef-forming organisms. The relatively short equilibration time of the surface ocean with atmospheric CO_2 implies a response time of Ω to increased CO_2 of only a few decades, comparable to the current acidification rate (see the Supplementary Materials). The current rate is probably a hundred times faster than at any time during the last hundreds of millennia (*93*), confirming the tied relations to transgression of the climate change boundary, leading to the rising risk of weakening ocean biosphere integrity, and worsening the aragonite saturation state of the ocean acidification boundary.

A systemic framework for addressing global anthropogenic impacts on Earth system

The scientific updates and analyses presented here confirm that humanity is today placing unprecedented pressure on Earth system. Perhaps most worrying in terms of maintaining Earth system in a Holocene-like interglacial state is that all the biosphere-related planetary boundary processes providing the resilience (capacity to dampen disturbance) of Earth system are at or close to a high-risk level of transgression. In a recent study (*18*), it was shown that several regional climate tipping points, relevant for stabilizing the global system, have already been or are close to being transgressed, thus weakening global resilience capacity. This implies low/falling resilience precisely when planetary resilience is needed more than ever to cope with increasing anthropogenic disturbances. There is an urgent need for more powerful scientific and policy tools for analyzing the whole of the integrated Earth system with reliability and regularity and guiding political processes to prevent altering the state of Earth system beyond levels tolerable for today's societies. In addition to more consistent collection and collation of relevant global environmental data, this will require the development of Earth system models that more completely capture geosphere-biosphere-anthroposphere interactions than is the case today. The known interdependence of planetary boundaries is confirmed by Earth system science understanding (*14*, *22*) of the planet as an integrated, partially self-regulating, system. To better understand the risk to this system and the critical boundaries that humankind should consider in its economic and social activities, Earth system analysis now has to continue advancing a planetary boundaries framework. In addition, it must substantially increase the ecological realism of simulation and analyses of the biosphere as an adaptive core entity of Earth system. These initiatives are underway but have to be further developed into a coherent process of integrated Earth system analysis across the physical, chemical, and biological domains not focused just on climate.

Successfully addressing anthropogenic climate change will require consideration of internal biosphere-geosphere interactions within Earth system. Our model results demonstrate that one of the most powerful means that humanity has at its disposal to combat climate change is respecting the land system change boundary. Bringing total global forest cover back to the levels of the late 20th century would provide a substantial cumulative sink for atmospheric CO_2 in 2100. This reforestation seems unlikely, however, given the current focus on biomass as a replacement for fossil fuels and the creation of negative CO_2 emissions via bioenergy with carbon capture and storage. Both activities are already serving to increase pressure on Earth's remaining forest area. Nevertheless, our study indicates that failure to respect the land system change planetary boundary can potentially jeopardize efforts to achieve the global climate goals adopted in the Paris Agreement.

Meanwhile, this update of the planetary boundaries framework may serve as a renewed wake-up call to humankind that Earth is in danger of leaving its Holocene-like state. It may also contribute to guiding the substantial human opportunities for sustainable development on our planet. Scientific insight into planetary boundaries does not limit, but stimulates, humankind to innovation toward a future in which Earth system stability is fundamentally preserved and safeguarded.

MATERIALS AND METHODS

To quantify the aerosol boundary, we consider cases where a natural pulse of sulfate aerosol emissions from volcanic eruptions in the northern hemisphere led to subsequent rainfall deficits in the Sahel. The eruption of El Chichón led to a peak interhemispheric AOD difference of 0.07 and that of Katmai to an AOD difference of 0.08 (*55*). We also consider a model study of intentional sulfate injections into the stratosphere. This study is based on stratospheric aerosols, which have no direct interaction with clouds and vegetation. However, it does indicate that an interhemispheric sulfate AOD difference of ~0.2 would decrease tropical monsoon precipitation in the northern hemisphere by ~10% and India's mean precipitation by >20% (*59*). Together, these studies suggest that a raised interhemispheric AOD difference caused by persistent and widely distributed aerosol emissions could lead to major reductions in precipitation in the tropics.

To examine differing scenarios of transgression of land system and climate change boundaries, we use the POEM [(*85*) and the Supplementary Materials], which links models of atmospheric

and ocean circulation with models of the marine (BLING) (*94*) and terrestrial biosphere (LPJmL5) [(*95*) and the Supplementary Materials]. We study scenarios where each of these two planetary boundary dimensions are either fixed at the value of the boundary, a value in the zone of increasing risk, or a value in the high-risk zone. Once the respective scenario condition is attained, the associated level of scenario forcing remains constant, while the long-term implications under these fixed conditions evolve. Correspondingly, vegetation dynamics (e.g., biome distributions) and related carbon pools and fluxes develop according to biophysical climate interactions under the given forcing conditions, while biogeochemical feedbacks on the atmosphere are not considered because of the respective boundary or transgression forcing remaining fixed.

Supplementary Materials

This PDF file includes:

Supplementary Information
Figs. S1 to S9
Tables S1 to S3
References

REFERENCES AND NOTES

1. J. Rockström, W. Steffen, K. Noone, Å. Persson, S. Chapin, E. F. Lambin, T. M. Lenton, M. Scheffer, C. Folke, J. Schellnhuber, B. Nykvist, C. A. DeWit, T. Hughes, S. van der Leeuw, H. Rodhe, S. Sörlin, P. K. Snyder, R. Costanza, U. Svedin, M. Falkenmark, L. Karlberg, R. W. Corell, V. J. Fabry, J. Hansen, D. Liverman, K. Richardson, P. Crutzen, J. Foley, A safe operating space for humanity. *Nature* **461**, 472–475 (2009).
2. W. Steffen, K. Richardson, J. Rockström, S. E. Cornell, I. Fetzer, E. M. Bennett, R. Biggs, S. R. Carpenter, W. de Vries, C. A. de Wit, C. Folke, D. Gerten, J. Heinke, G. M. Mace, L. M. Persson, V. Ramanathan, B. Reyers, S. Sörlin, Planetary boundaries: Guiding human development on a changing planet. *Science* **347**, 1259855 (2015).
3. W. Steffen, K. Richardson, J. Rockström, H. Schellnhuber, O. P. Dube, S. Dutreil, T. M. Lenton, J. Lubchenco, The emergence and evolution of Earth system science. *Nat. Rev. Earth Environ.* **1**, 54–63 (2020).
4. J. Zalasiewicz, C. N. Waters, C. Summerhayes, A. P. Wolfe, A. D. Barnosky, A. Cearreta, P. Crutzen, E. C. Ellis, J. J. Fairchild, A. Gałuszka, P. Haff, I. Hajdas, M. J. Head, J. A. I. do Sul, C. Jeandel, R. Leinfelder, J. R. McNeill, C. Neal, E. Odada, N. Oreskes, W. Steffen, J. P. M. Syvitski, M. Wagreich, M. Williams, The working group on the 'Anthropocene': Summary of evidence and recommendations. *Anthropocene* **19**, 55–60 (2017).
5. C. N. Waters, J. Zalasiewicz, C. Summerhayes, A. D. Barnosky, C. Poirier, A. Gałuszka, A. Cearreta, M. Edgeworth, E. C. Ellis, M. Ellis, C. Jeandel, R. Leinfelder, J. R. McNeill, D. D. Richter, W. Steffen, J. Syvitski, D. Vidas, M. Wagreich, M. Williams, A. Zhisheng, J. Grinevald, E. Odada, N. Oreskes, A. P. Wolfe, The Anthropocene is functionally and stratigraphically distinct from the Holocene. *Science* **351**, eaad2622 (2016).
6. W. F. Ruddiman, *Earth's Climate: Past and Future* (Third edition, W.H. Freeman and Co., 2014).
7. C. P. Summerhayes, *Paleoclimatology: From Snowball Earth to the Anthropocene* (Wiley-Blackwell, 2020).
8. H.-J. Schellnhuber, Discourse: Earth system analysis—The scope of the challenge, in *Earth System Analysis: Integrating Science for Sustainability*. H.-J. Schellnhuber, V. Wenzel, Eds. (Springer, Heidelberg, 1998), pp. 3–195.
9. M. B. Osman, J. E. Tierney, J. Zhu, R. Tardif, G. J. Hakim, J. King, C. J. Poulsen, Globally resolved surface temperatures since the Last Glacial Maximum. *Nature* **599**, 239–244 (2021).
10. R. M. Beyer, M. Krapp, A. Manica, High-resolution terrestrial climate, bioclimate and vegetation for the last 120,000 years. *Sci. Data.* **7**, 236 (2020).
11. P. K. Snyder, C. Delire, J. A. Foley, Evaluating the influence of different vegetation biomes on the global climate. *Clim. Dyn.* **23**, 279–302 (2004).
12. P. C. West, G. T. Narisma, C. C. Barford, C. J. Kucharik, J. A. Foley, An alternative approach for quantifying climate regulation by ecosystems. *Front. Ecol. Environ.* **9**, 126–133 (2010).
13. S. J. Lade, W. Steffen, W. de Vries, S. R. Carpenter, J. F. Donges, D. Gerten, H. Hoff, T. Newbold, K. Richardson, J. Rockström, Human impacts on planetary boundaries amplified by Earth system interactions. *Nat. Sustain.* **3**, 119–128 (2020).
14. A. Chrysafi, V. Virkki, M. Jalava, V. Sandström, J. Piipponen, M. Porkka, S. Lade, K. La Mere, L. Wang-Erlandsson, L. Scherer, L. Andersen, E. Bennett, K. Brauman, G. Cooper, A. De Palma, P. Döll, A. Downing, T. DuBois, I. Fetzer, E. Fulton, D. Gerten, H. Jaafar, J. Jaegermeyr, F. Jaramillo, M. Jung, H. Kahiluoto, A. Mackay, L. Lassaletta, D. Mason-D'Croz, M. Mekonnen, K. Nash, A. Pastor, N. Ramankutty, B. Ridoutt, S. Siebert, B. Simmons, A. Staal, Z. Sun, A. Tobian, A. Usubiaga-Liaño, R. van der Ent, A. van Soesbergen, P. Verburg, Y. Wada, S. Zipper, M. Kummu, Quantifying Earth system interactions for sustainable food production: An expert elicitation. *Nat. Sustain.* **5**, 830–842 (2022).
15. Intergovernmental Panel on Climate Change, *Climate Change 2022: Impacts, Adaptation, and Vulnerability*, H.-O. Pörtner, D. C. Roberts, M. Tignor, E. S. Poloczanska, K. Mintenbeck, A. Alegría, M. Craig, S. Langsdorf, S. Löschke, V. Möller, A. Okem, B. Rama, Eds. (Cambridge Univ. Press, 2022).
16. E. S. Brondizio, J. Settele, S. Díaz, H. T. Ngo, *Global Assessment Report on Biodiversity and Ecosystem Services of the Intergovernmental Science-Policy Platform on Biodiversity and Ecosystem Services* (IPBES, 2019).
17. Intergovernmental Panel on Climate Change, *Climate Change 2021: The Physical Science Basis* (Cambridge University Press, 2021).
18. D. A. McKay, A. Staal, J. Abrams, R. Winkelmann, B. Sakschewski, S. Loriani, I. Fetzer, S. E. Cornell, J. Rockström, T. M. Lenton, Exceeding 1.5°C global warming could trigger multiple climate tipping points. *Science* **377**, eabn7950 (2022).
19. Past Interglacials Working Group of PAGES, Interglacials of the last 800,000 years. *Rev. Geophys.* **54**, 162–219 (2016).
20. C. Ragon, V. Lembo, V. Lucarini, C. Vérard, J. Kasparian, M. Brunetti, Robustness of competing climatic states. *J. Clim.* **35**, 2769–2784 (2022).
21. J. M. Anderies, S. R. Carpenter, W. Steffen, J. Rockström, The topology of non-linear global carbon dynamics: From tipping points to planetary boundaries. *Environ. Res. Lett.* **8**, 044048 (2013).
22. S. J. Lade, J. Norberg, J. Anderies, C. Beer, S. Cornell, J. Donges, I. Fetzer, T. Gasser, K. Richardson, J. Rockström, W. Steffen, Potential feedbacks between loss of biosphere integrity and climate change. *Glob. Sust.* **2**, 1–15 (2019).
23. M. Exposito-Alonso, T. R. Booker, L. Czech, T. Fukami, L. Gillespie, S. Hateley, C. C. Kyriazis, P. L. M. Lang, L. Leventhal, D. Nogues-Bravo, V. Pagowski, M. Ruffley, J. P. Spence, S. E. Toro Arana, C. L. Weiß, E. Zess, Genetic diversity loss in the Anthropocene. *Science* **377**, 1431–1435 (2022).
24. H. Ceballos, P. R. Ehrlich, A. D. Barnosky, A. García, R. M. Pringle, T. M. Palmer, Accelerated modern human–induced species losses: Entering the sixth mass extinction. *Sci. Adv.* **1**, e1400253 (2015).
25. M. D. A. Rounsevell, M. Harfoot, P. A. Harrison, T. Newbold, R. D. Gregory, G. M. Mace, A biodiversity target based on species extinctions. *Science* **368**, 1193–1195 (2020).
26. R. H. Cowie, P. Bouchet, B. Fontaine, The sixth mass extinction: Fact, fiction or speculation? *Biol. Rev.* **97**, 640–663 (2022).
27. R. J. Scholes, R. Biggs, A Biodiversity Intactness Index. *Nature* **434**, 45–49 (2005).
28. P. A. Martin, R. E. Green, A. Balmford, The Biodiversity Intactness Index may underestimate losses. *Nat. Evol.* **3**, 862–863 (2019).
29. S. E. Jorgensen, Y. M. Svirezhev, *Towards a Thermodynamic Theory for Ecological Systems* (Elsevier, 2004).
30. A. Kleidon, Sustaining the terrestrial biosphere in the anthropocene: A thermodynamic Earth system perspective. *Ecol. Economy Soc. INSEE J.* **6**, 53–80 (2023).
31. S. W. Running, A measurable planetary boundary for the biosphere. *Science* **337**, 1458–1459 (2012).
32. H. Haberl, K. H. Erb, F. Krausmann, Human appropriation of net primary production: Patterns, trends, and planetary boundaries. *Annu. Rev. Environ. Res.* **39**, 363–391 (2014).
33. F. Krausmann, K. H. Erb, S. Gingrich, H. Haberl, A. Bondeau, V. Gaube, C. Lauka, C. Plutzar, T. D. Searchinger, Global human appropriation of net primary production doubled in the 20th century. *Proc. Natl. Acad. Sci. U.S.A.* **110**, 10324–10329 (2013).
34. L. V. Gatti, L. S. Basso, J. B. Miller, M. Gloor, L. G. Dominigues, H. L. G. Cassol, G. Tejada, L. E. O. C. Aragao, C. Nobre, W. Peters, L. Marani, E. Arai, A. H. Sanches, S. M. Correa, L. Anderson, C. Von Randow, C. S. C. Correia, S. P. Crispim, R. A. L. Neves, Amazonia as a carbon source linked to deforestation and climate change. *Nature* **595**, 388–393 (2021).
35. K. Goldewijk, A. Beusen, J. Doelman, E. Stehfest, Anthropogenic land use estimates for the Holocene – HYDE 3.2. *Earth Syst. Sci. Data* **9**, 927–953 (2017).
36. D. Gerten, V. Heck, J. Jägermeyr, B. L. Bodirsky, I. Fetzer, M. Jalava, M. Kummu, W. Lucht, J. Rockström, S. Schaphoff, H. J. Schellnhuber, Feeding ten billion people is possible within four terrestrial planetary boundaries. *Nat. Sust.* **3**, 200–208 (2020).
37. S. Ostberg, W. Lucht, S. Schaphoff, D. Gerten, Critical impacts of global warming on land ecosystems. *Earth Syst. Dyn.* **4**, 347–357 (2013).
38. W. Schwartz, E. Sala, S. Tracey, R. Watson, D. Pauly, The spatial expansion and ecological footprint of fisheries (1950 to present). *PLOS ONE* **5**, e15143 (2010).

39. J. S. Link, R. A. Watson, Global ecosystem overfishing: Clear delineation within real limits to production. *Sci. Adv.* **5**, eaav047 (2019).
40. B. Planque, J.-M. Fromentin, P. Cury, K. F. Drinkwater, S. Jennings, R. I. Perry, S. Kifani, How does fishing alter marine populations and ecosystems sensitivity to climate? *J. Mar. Sys.* **79**, 403–417 (2010).
41. P. M. Forster, C. J. Smith, T. Walsh, W. F. Lamb, M. D. Palmer, K. von Schuckmann, B. Trewin, M. Allen, R. Andrew, A. Birt, A. Borger, T. Boyer, J. A. Broersma, L. Cheng, F. Dentener, P. Friedlingstein, N. Gillett, J. M. Gutiérrez, J. Gütschow, M. Hauser, B. Hall, M. Ishii, S. Jenkins, R. Lamboll, X. Lan, J.-Y. Lee, C. Morice, C. Kadow, J. Kennedy, R. Killick, J. Minx, V. Naik, G. Peters, A. Pirani, J. Pongratz, A. Ribes, J. Rogelj, D. Rosen, C.-F. Schleussner, S. Seneviratne, S. Szopa, P. Thorne, R. Rohde, M. Rojas Corradi, D. Schumacher, R. Vose, K. Zickfeld, X. Zhang, V. Masson-Delmotte, P. Zhai, Indicators of Global Climate Change 2022: Annual update of large-scale indicators of the state of the climate system and the human influence. *Earth Syst. Sci. Data* **15**, 2295–2327 (2023).
42. H. Schellnhuber, S. Rahmstorf, R. Winkelmann, Why the right climate target was agreed in Paris. *Nat. Clim. Change* **6**, 649–653 (2016).
43. L. Persson, B. Almroth, C. Collins, S. Cornell, C. de Wit, M. Diamond, P. Fantke, M. Hassellöv, M. MacLeod, M. Ryberg, P. Jørgensen, P. Villarrubia-Gómez, Z. Wang, M. Zwicky Hauschild, Outside the safe operating space of the planetary boundary for novel entities. *Environ. Sci. Tech.* **56**, 1510–1521 (2022).
44. P. J. Nair, L. Froidevaux, J. Kuttippurath, J. M. Zawodny, J. M. Russell III, W. Steinbrecht, H. Claude, T. Leblanc, J. A. E. van Gijsel, B. Johnson, D. P. J. Swart, A. Thomas, R. Querel, R. Wang, J. Anderson, Subtropical and midlatitude ozone trends in the stratosphere: Implications for recovery. *J. Geophys. Res. Atmos.* **120**, 7247–7257 (2015).
45. A. Pazmiño, S. Godin-Beekmann, A. Hauchecorne, C. Claud, S. Khaykin, F. Goutail, E. Wolfram, J. Salvador, E. Quel, Multiple symptoms of total ozone recovery inside the Antarctic vortex during austral spring. *Atmospheric Chem. Phys.* **18**, 7557–7572 (2018).
46. M. Porkka, V. Virkki, L. Wang-Erlandsson, D. Gerten, T. Gleeson, C. Mohan, I. Fetzer, F. Jaramillo, A. Staal, S. te Wierik, A. Tobian, R. van der Ent, P. Döll, M. Flörke, S. N. Gosling, N. Hanasaki, Y. Satoh, H. M. Schmied, N. Wanders, J. Rockström, M. Kummu, Global water cycle shifts far beyond pre-industrial conditions – Planetary boundary for freshwater change transgressed (2023); https://eartharxiv.org/repository/view/3438/.
47. T. Gleeson, L. Wang-Erlandsson, S. C. Zipper, M. Porkka, F. Jaramillo, D. Gerten, I. Fetzer, S. E. Cornell, L. Piemontese, L. J. Gordon, J. Rockström, T. Oki, M. Sivapalan, Y. Wada, K. A. Brauman, M. Flörke, M. F. P. Bierkens, B. Lehner, P. Keys, M. Kummu, T. Wagener, S. Dadson, T. J. Troy, W. Steffen, M. Falkenmark, J. S. Famiglietti, The water planetary boundary: Interrogation and revision. *One Earth.* **2**, 223–234 (2020).
48. L. Wang-Erlandsson, A. Tobian, R. J. van der Ent, I. Fetzer, S. te Wierik, M. Porkka, A. Staal, F. Jaramillo, H. Dahlmann, C. Singh, P. Greve, D. Gerten, P. W. Keys, T. Gleeson, S. E. Cornell, W. Steffen, X. Bai, J. Rockström, A planetary boundary for green water. *Nat. Rev. Earth Environ.* **3**, 380–392 (2022).
49. Y. Qin, N. D. Mueller, S. Siebert, R. B. Jackson, A. A. Kouchak, J. B. Zimmerman, D. Tong, C. Hong, S. J. Davis, Flexibility and intensity of global water use. *Nat. Sustain.* **2**, 515–523 (2019).
50. K. S. Carslaw, H. Gordon, D. S. Hamilton, J. S. Johnson, L. A. Regayre, M. Yoshioka, K. J. Pringle, Aerosols in the pre-industrial atmosphere. *Curr. Clim. Chang. Rep.* **3**, 1–15 (2017).
51. N. Bellouin, J. Quaas, E. Gryspeerdt, S. Kinne, P. Stier, D. Watson-Parris, O. Boucher, K. S. Carslaw, M. Christensen, A.-L. Daniau, J.-L. Dufresne, G. Feingold, S. Fiedler, P. Forster, A. Gettelman, J. M. Haywood, U. Lohmann, F. Malavelle, T. Mauritsen, D. T. McCoy, G. Myhre, J. Mülmenstädt, D. Neubauer, A. Possner, M. Rugenstein, Y. Sato, M. Schulz, S. E. Schwartz, O. Sourdeval, T. Storelvmo, V. Toll, D. Winker, B. Stevens, Bounding global aerosol radiative forcing of climate change. *Rev. Geophys.* **58**, e2019RG000660 (2020).
52. J. Hooper, S. K. Marx, A global doubling of dust emissions during the Anthropocene? *Glob. Planet. Change* **169**, 70–91 (2018).
53. P. Kinppertz, M. C. Todd, Mineral dust aerosols over the Sahara: Meteorological controls on emission and transport and implications for modeling. *Rev. Geophys.* **50**, RG1007 (2012).
54. M. L. Griffiths, K. R. Johnson, F. S. R. Pausata, J. C. White, G. M. Henderson, C. T. Wood, H. Yang, V. Ersek, C. Conrad, N. Sekhon, End of Green Sahara amplified mid- to late Holocene megadroughts in mainland Southeast Asia. *Nat. Commun.* **11**, 4204 (2020).
55. M. Chin, T. Diehl, Q. Tan, J. M. Prospero, R. A. Kahn, L. A. Remer, H. Yu, A. M. Sayer, H. Bian, I. V. Geogdzhayev, B. N. Holben, S. G. Howell, B. J. Huebert, N. C. Hsu, D. Kim, T. L. Kucsera, R. C. Levy, M. I. Mishchenko, X. Pan, P. K. Quinn, G. L. Schuster, D. G. Streets, S. A. Strode, O. Torres, X.-P. Zhao, Multi-decadal aerosol variations from 1980 to 2009: A perspective from observations and a global model. *Atmos. Chem. Phys.* **14**, 3657–3690 (2014).
56. L. Sogacheva, T. Popp, A. M. Sayer, O. Dubovik, M. J. Garay, A. Heckel, N. C. Hsu, H. Jethva, R. A. Kahn, P. Kolmonen, M. Kosmale, G. de Leeuw, R. C. Levy, P. Litvinov, A. Lyapustin, P. North, O. Torres, Merging regional and global AOD records from 15 available satellite products. *Atmos. Chem. Phys.* **20**, 2031–2056 (2019).
57. A. Vogel, G. Alessa, R. Scheele, L. Weber, O. Dubovik, P. North, S. Fiedler, Uncertainty in aerosol optical depth from modern aerosol-climate models, reanalyses, and satellite products. *J. Geophys. Res. Atmos.* **127**, e2021JD035483 (2022).
58. J. Haywood, A. Jones, N. Bellouin, D. Stephenson, Asymmetric forcing from stratospheric aerosols impacts Sahelian rainfall. *Nat. Clim. Change.* **3**, 660–665 (2013).
59. K. S. Krishnamohan, G. Bala, Sensitivity of tropical monsoon precipitation to the latitude of stratospheric aerosol injections. *Clim. Dyn.* **59**, 151–168 (2022).
60. S. Roose, G. Bala, K. S. Krishnamohan, L. Cao, K. Caldeira, Quantification of tropical monsoon precipitation changes in terms of interhemispheric differences in stratospheric sulfate aerosol optical depth. *Clim. Dyn.* **2023**, 1–16 (2023).
61. A. Donohoe, J. Marshall, D. Ferreira, D. Mcgee, The relationship between ITCZ location and cross-equatorial atmospheric heat transport: From the seasonal cycle to the last glacial maximum. *J. Clim.* **26**, 3597–3618 (2013).
62. M. C. MacCracken, H.-J. Shin, K. Caldeira, G. A. Ban-Weiss, Climate response to imposed solar radiation reductions in high latitudes. *Earth Syst. Dyn.* **4**, 301–315 (2013).
63. N. Devaraju, G. Bala, A. Modak, Effects of large-scale deforestation on precipitation in the monsoon regions: Remote versus local effects. *Proc. Natl. Acad. Sci. U.S.A.* **112**, 3257–3262 (2015).
64. I. B. Ocko, V. Ramaswamy, Y. Ming, Contrasting climate responses to the scattering and absorbing features of anthropogenic aerosol forcings. *J. Clim.* **27**, 5329–5345 (2014).
65. M. Zhao, L. Cao, G. Bala, L. Duan, Climate response to latitudinal and altitudinal distribution of stratospheric sulfate aerosols. *J. Geophys. Res. Atmos.* **126**, e2021JD035379 (2021).
66. J. T. Fasullo, B. L. Otto-Bliesner, S. Stevenson, The influence of volcanic aerosol meridional structure on monsoon responses over the last millennium. *Geophys. Res. Lett.* **46**, 12350–12359 (2019).
67. S. Fiedler, T. Crueger, R. D'Agostino, K. Peters, T. Becker, D. Leutwyler, L. Paccini, J. Burdanowitz, S. Buehler, A. Uribe, T. Dauhut, D. Dommenget, K. Fraedrich, L. Jungandreas, N. Maher, A. Naumann, M. Rugenstein, M. Sakradzija, H. Schmidt, F. Sielmann, C. Stephan, C. Timmreck, X. Zhu, B. Stevens, Simulated tropical precipitation assessed across three major phases of the Coupled Model Intercomparison Project (CMIP). *Mon. Weather Rev.* **148**, 3653–3680 (2020).
68. P. Zanis, D. Akritidis, A. K. Georgoulias, R. J. Allen, S. E. Bauer, O. Boucher, J. Cole, B. Johnson, M. Deushi, M. Michou, J. Mulcahy, P. Nabat, D. Olivié, N. Oshima, A. Sima, M. Schulz, T. Takemura, K. Tsigaridis, Fast responses on pre-industrial climate from present-day aerosols in a CMIP6 multi-model study. *Atmos. Chem. Phys.* **20**, 8381–8404 (2020).
69. S. Fiedler, B. Stevens, M. Gidden, S. J. Smith, K. Riahi, D. van Vuuren, First forcing estimates from the future CMIP6 scenarios of anthropogenic aerosol optical properties and an associated Twomey effect. *Geosci. Model Dev.* **12**, 989–1007 (2019).
70. N. M. Mahowald, R. Scanza, J. Brahney, C. L. Goodale, P. G. Hess, J. K. Moore, J. Neff, Aerosol deposition impacts on land and ocean carbon cycles. *Curr. Clim. Change Rep.* **3**, 16–31 (2017).
71. L. Jiang, R. A. Feely, B. R. Carter, D. J. Greeley, D. K. Gledhill, K. M. Arzayus, Climatological distribution of aragonite saturation state in the global oceans. *Glob. Biogeochem. Cycles.* **29**, 1656–1673 (2015).
72. EU Copernicus Climate Change Service, "Land cover classification gridded maps from 1992 to present derived from satellite observations", ICDR Land Cover 2016–2020.
73. Food and Agricultural Organization of the United Nations, (FAO), United Nations' Environmental Program, (UNEP), "The State of the World's Forests 2020. Forests, biodiversity and people" (Publication 978-92-5-132419-6, 2020); https://doi.org/10.4060/ca8642en.
74. Food and Agricultural Organization of the United Nations, (FOA), "Global Forest Resources Assessment 2020: Main report" (Publication 978-92-5-132974-0, 2020); https://doi.org/10.4060/ca9825en.
75. S. R. Carpenter, E. M. Bennett, Reconsideration of the planetary boundary for phosphorus. *Environ. Res. Lett.* **6**, 014009 (2011).
76. C. Liu, H. Tian, Global nitrogen and phosphorus fertilizer use for agriculture production in the past half century: Shifted hot spots and nutrient imbalance. *Earth Syst. Sci. Data* **9**, 181–192 (2017).
77. W. J. Brownlie, M. A. Sutton, K. V. Heal, D. S. Reay, B. M. Spears (eds.), *Our Phosphorus Future* (U.K. Centre for Ecology & Hydrology, 2022).
78. T. Zou, X. Zhang, E. Davidson, Improving phosphorus use efficiency in cropland to address phosphorus challenges by 2050. *Earth Space Sci. Open Archive*, (2020). https://doi.org/10.1002/essoar.10504095.1
79. D. Cordell, S. White, Life's bottleneck: Sustaining the World's phosphorus for a food secure future. *Annu. Rev. Environ. Res.* **39**, 161–188 (2014).
80. Food and Agriculture Organisation of the United Nations (FAO), "World fertilizer trends and outlook to 2022 – Summary Report, Rome" (2019); www.fao.org/3/ca6746en/ca6746en.pdf)

81. M. A. Adams, N. Buchmann, J. Sprent, T. N. Buckley, T. L. Turnbull, Crops, nitrogen, water: Are legumes friend, foe, or misunderstood ally? *Trends Plant. Sci.* **23**, 539–550 (2018).
82. P. M. Vitousek, D. N. L. Menge, S. C. Reed, C. C. Cleveland, Biological nitrogen fixation: Rates, patterns and ecological controls in terrestrial ecosystems. *Philos. Trans. R. Soc. Lond. B. Biol. Sci.* **368**, 1621 (2013).
83. M. V. B. Figueiredo, A. E. S. Mergulhão, J. K. Sobral, M. A. L. Junio, A. S. F. Araújo, Biological nitrogen fixation: Importance, associated diversity, and estimates, in *Plant Microbe Symbiosis: Fundamentals and Advances* (Springer, 2013), pp. 267–289.
84. FAO, "FAOSTAT—FAO database for food and agriculture" (2022); www.fao.org/faostat/ (accessed 4.19.22)
85. M. Drüke, W. von Bloh, S. Petri, B. Sakschewski, S. Schaphoff, M. Forkel, W. Huiskamp, G. Feulner, K. Thonicke, CM2Mc-LPJmL v1.0: Biophysical coupling of a process-based dynamic vegetation model with managed land to a general circulation model. *Geosci. Model. Dev.* **14**, 4117–4141 (2021).
86. K.-H. Erb, T. Kastner, C. Plutzar, A. L. S. Bais, N. Carvalhais, T. Fetzel, S. Gingrich, H. Haberl, C. Lauk, M. Niedertscheider, J. Pongratz, M. Thurner, S. Luyssaert, Unexpectedly large impact of forest management and grazing on global vegetation biomass. *Nature* **553**, 73–76 (2017).
87. Y. M. Bar-On, R. Phillips, R. Milo, The biomass distribution on Earth. *Proc. Natl. Acad. Sci. U.S.A.* **115**, 6506–6511 (2018).
88. K. Matsuomoto, T. Hashioka, Y. Yamanaka, Effect of temperature-dependent organic carbon decay on atmospheric pCO_2. *J. Geophys. Res.* **112**, G02007 (2007).
89. L. Kwiatkowski, O. Torres, L. Bopp, O. Aumont, M. Chamberlain, J. R. Christian, J. P. Dunne, M. Gehlen, T. Ilyina, J. G. John, A. Lenton, H. Li, N. S. Lovenduski, J. C. Orr, J. Palmieri, Y. Santana-Falcón, J. Schwinger, R. Séférian, C. A. Stock, A. Tagliabue, Y. Takano, J. Tjiputra, K. Toyama, H. Tsujino, M. Watanabe, A. Yamamoto, A. Yool, T. Ziehn, Twenty-first century ocean warming, acidification, deoxygenation, and upper-ocean nutrient and primary production decline from CMIP6 model projections. *Biogeosci* **17**, 3439–3470 (2020).
90. E. A. Laws, E. D'Sa, P. Naik, Simple equations to estimate ratios of new or export production to total production from satellite-derived estimates of sea surface temperature and primary production. *Limnol. Oceanogr. Meth.* **9**, 593–601 (2011).
91. C. M. Marsay, R. J. Sanders, S. A. Henson, K. Pabortsava, E. P. Achterberg, R. S. Lampitt, Attenuation of sinking POC flux in the mesopelagic. *Proc. Natl. Acad. Sci. U.S.A.* **112**, 1089–1094 (2015).
92. K. A. Chrichton, J. D. Wilson, A. Ridgewell, F. Boscob-Galazzo, E. H. John, B. S. Wade, P. N. Pearson, What the geological past can tell us about the future of the ocean's twilight zone. *Nat. Commun.* **14**, 2376 (2023).
93. The Royal Society, "Ocean acidification due to increasing atmospheric carbon dioxide" (Publication 0 85403 617 2, Policy Doc. 12/05, R. Soc., 2005).
94. E. D. Galbraith, J. P. Dunne, A. Gnanadesikan, R. D. Slater, J. L. Sarmiento, C. O. Dufour, G. F. de Souza, D. Bianchi, M. Claret, K. B. Rodgers, S. S. Marvasti, Complex functionality with minimal computation: Promise and pitfalls of reduced-tracer ocean biogeochemistry models. *J. Adv. Model Earth Syst.* **7**, 2012–2028 (2015).
95. S. Schaphoff, M. Forkel, C. Müller, J. Knauer, W. von Bloh, D. Gerten, J. Jägermeyr, W. Lucht, A. Rammig, K. Thonicke, K. Waha, LPJmL4 – A dynamic global vegetation model with managed land – Part 2: Model evaluation. *Geosci. Model Dev.* **11**, 1377–1403 (2018b).
96. NASA Earth Observation, "AURA Ozone data"; https://neo.gsfc.nasa.gov/archive/geotiff.float/AURA_OZONE_M/.
97. N. Ramankutty, J. A. Foley, Characterizing patterns of global land use: An analysis of global croplands data. *Glob. Biogeochem. Cycles.* **12**, 667–685 (1998).
98. C. W. Snyder, M. D. Mastrandrea, S. H. Schneider, The complex dynamics of the climate system: Constraints on our knowledge, policy implications and the necessity of systems thinking. *Philos. Complex Syst.* **10**, 467–505 (2011).
99. M. Willeit, A. Ganopolski, R. Calov, V. Brovkin, Mid-Pleistocene transition in glacial cycles explained by declining CO_2 and regolith removal. *Sci. Adv.* **5**, eaav7337 (2019).
100. J. Zheng, J. L. Payne, A. Wagner, Cryptic genetic variation accelerates evolution by opening access to diverse adaptive peaks. *Science* **365**, 347–353 (2019).
101. M. C. Bitter, L. Kapsenberg, J.-P. Gattuso, C. A. Pfister, Standing genetic variation fuels rapid adaptation to ocean acidification. *Nat. Commun.* **10**, 5821 (2019).
102. T. H. Oliver, M. S. Heard, N. J. Isaac, D. B. Roy, D. Procter, F. Eigenbrod, R. Freckleton, A. Hector, C. D. L. Orme, O. L. Petchey, V. Proença, Biodiversity and resilience of ecosystem functions. *Trends Ecol. Evol.* **30**, 673–684 (2015).
103. A. A. Hoffmann, C. M. Sgrò, T. N. Kristensen, Revisiting adaptive potential, population size, and conservation. *Trends Ecol. Evol.* **32**, 506–517 (2017).
104. A. Miraldo, S. Li, M. K. Borregaard, A. Flórez-Rodríguez, S. Gopalakrishnan, M. Rizvanovic, Z. Wang, C. Rahbek, K. A. Marske, D. Nogués-Bravo, An anthropocene map of genetic diversity. *Science* **353**, 1532–1535 (2016).
105. S. Blanchet, J. G. Prunier, H. De Kort, Time to go bigger: Emerging patterns in macrogenetics. *Trends Genet.* **33**, 579–580 (2017).
106. S. Theodoridis, D. A. Fordham, S. C. Brown, S. Li, C. Rahbek, D. Nogues-Bravo, Evolutionary history and past climate change shape the distribution of genetic diversity in terrestrial mammals. *Nat. Commun.* **11**, 2557 (2020).
107. D. M. Leigh, C. B. van Rees, K. L. Millette, M. F. Breed, C. Schmidt, L. D. Bertola, B. K. Hand, M. E. Hunter, E. L. Jensen, F. Kershaw, L. Liggins, G. Luikart, S. Manel, J. Mergeay, J. M. Miller, G. Segelbacher, S. Hoban, I. Paz-Vinas, Opportunities and challenges of macrogenetic studies. *Nat. Rev. Genet.* **22**, 791–807 (2021).
108. S. Theodoridis, C. Rahbek, D. Nogués-Bravo, Exposure of mammal genetic diversity to mid-21st century global change. *Ecography* **44**, 817–831 (2021).
109. S. Hoban, M. Brufordb, J. D'Urban Jackson, M. Lopes-Fernandes, M. Heuertz, P. A. Hohenlohe, I. Paz-Vinas, P. Sjögren-Gulve, G. Segelbacher, C. Vernesi, S. Aitken, L. D. Bertola, P. Bloomer, M. Breed, H. Rodríguez-Correa, W. C. Funk, C. E. Grueber, M. E. Hunter, L. Laikre, Genetic diversity targets and indicators in the CBD post-2020 global biodiversity framework must be improved. *Biol. Conserv.* **248**, 108654 (2020).
110. A. Ganopolski, V. Brovkin, Simulation of climate, ice sheets and CO_2 evolution during the last four glacial cycles with an Earth system model of intermediate complexity. *Clim.* **13**, 1695–1716 (2017).
111. S. Schaphoff, W. Bloh, A. Rammig, K. Thonicke, H. Biemans, M. Forkel, D. Gerten, J. Heinke, J. Jägermeyr, J. Knauer, F. Langerwisch, W. Lucht, C. Müller, S. Rolinski, K. Waha, LPJmL4–a dynamic global vegetation model with managed land – Part 1: Model description. *Geosci. Model Dev.* **11**, 1343–1375 (2018).
112. I. C. Harris, P. D. Jones, "CRU TS3.23: Climatic Research Unit (CRU) Time-Series (TS) Version 3.23 of High Resolution Gridded Data of Month-by-month Variation in Climate (Jan. 1901-Dec. 2014)" (CEDA Archive, 2015); https://catalogue.ceda.ac.uk/uuid/5dca9487dc614711a3a933e44a933ad3
113. I. Harris, P. Jones, T. Osborn, D. Lister, Updated high-resolution grids of monthly climatic observations – The CRU TS3.10 dataset. *Int. J. Climatol.* **34**, 623–642 (2014).
114. D. Kaufman, N. McKay, C. Routson, M. Erb, C. Dätwyler, P. S. Sommer, O. Heiri, B. Davis, Holocene global mean surface temperature, a multi-method reconstruction approach. *Sci. Data* **7**, 201 (2020).
115. H. Haberl, K. H. Erb, F. Krausmann, V. Gaube, A. Bondeau, C. Plutzar, S. Gingrich, W. Lucht, M. Fischer-Kowalski, Quantifying and mapping the human appropriation of net primary production in Earth's terrestrial ecosystems. *Proc. Natl. Acad. Sci. U.S.A.* **104**, 12942–12947 (2007).
116. D. Lawrence, K. Vandecar, Effects of tropical deforestation on climate and agriculture. *Nat. Clim. Change* **5**, 27–36 (2015).
117. P. W. Keys, L. Wang-Erlandsson, L. J. Gordon, Revealing invisible water: Moisture recycling as an ecosystem service. *PLOS ONE* **11**, e0151993 (2016).
118. L. Wang-Erlandsson, I. Fetzer, P. W. Keys, R. J. van der Ent, H. H. G. Savenije, L. J. Gordon, Remote land use impacts on river flows through atmospheric teleconnections. *Hydrol. Earth Syst. Sci.* **22**, 4311–4328 (2018).
119. D. Gerten, H. Hoff, J. Rockström, J. Jägermeyr, M. Kummu, A. V. Pastor, Towards a revised planetary boundary for consumptive freshwater use: Role of environmental flow requirements. *Curr. Opin. Environ. Sustain.* **5**, 551–558 (2013).
120. J. Liu, C. Zang, S. Tian, J. Liu, H. Yang, S. Jia, L. You, B. Liu, M. Zhang, Water conservancy projects in China: Achievements, challenges and way forward. *Glob. Environ. Change* **23**, 633–643 (2013).
121. J. Sillmann, C. W. Stjern, G. Myhre, B. H. Samset, Ø. Hodnebrog, T. Andrews, O. Boucher, G. Faluvegi, P. Forster, M. R. Kasoar, V. V. Kharin, A. Kirkevåg, J.-F. Lamarque, D. J. L. Olivié, T. B. Richardson, D. Shindell, T. Takemura, A. Voulgarakis, F. W. Zwiers, Extreme wet and dry conditions affected differently by greenhouse gases and aerosols. *Nat. Clim. Atmospheric Sci.* **2**, 1–7 (2019).
122. N. L. Poff, J. D. Olden, D. M. Merritt, D. M. Pepin, Homogenization of regional river dynamics by dams and global biodiversity implications. *Proc. Natl. Acad. Sci. U.S.A.* **104**, 5732–5737 (2007).
123. A. Staal, O. A. Tuinenburg, J. H. C. Bosmans, M. Holmgren, E. H. van Nes, M. Scheffer, D. C. Zemp, S. C. Dekker, Forest-rainfall cascades buffer against drought across the Amazon. *Nat. Clim. Change* **8**, 539–543 (2018).
124. A. Günther, A. Barthelmes, V. Huth, H. Joosten, G. Jurasinski, F. Koebsch, J. Couwenberg, Prompt rewetting of drained peatlands reduces climate warming despite methane emissions. *Nat. Commun.* **11**, 1644 (2020).
125. T. Maavara, Q. Chen, K. Van Meter, L. E. Brown, J. Zhang, J. Ni, C. Zarfl, River dam impacts on biogeochemical cycling. *Nat. Rev. Earth Environ.* **1**, 103–116 (2020).
126. N. Boers, N. Marwan, H. M. J. Barbosa, J. Kurths, A deforestation-induced tipping point for the south American monsoon system. *Sci. Rep.* **7**, 41489 (2017).
127. K. Frieler, S. Lange, F. Piontek, C. P. O. Reyer, J. Schewe, L. Warszawski, F. Zhao, L. Chini, S. Denvil, K. Emanuel, T. Geiger, K. Halladay, G. Hurtt, M. Mengel, D. Murakami, S. Ostberg, A. Popp, R. Riva, M. Stevanovic, T. Suzuki, J. Volkholz, E. Burke, P. Ciais, K. Ebi, T. D. Eddy, J. Elliott, E. Galbraith, S. N. Gosling, F. Hattermann, T. Hickler, J. Hinkel, C. Hof, V. Huber,

J. Jägermeyr, V. Krysanova, R. Marcé, H. Müller Schmied, I. Mouratiadou, D. Pierson, D. P. Tittensor, R. Vautard, M. van Vliet, M. F. Biber, R. A. Betts, B. L. Bodirsky, D. Deryng, S. Frolking, C. D. Jones, H. K. Lotze, H. Lotze-Campen, R. Sahajpal, K. Thonicke, H. Tian, Y. Yamagata, Assessing the impacts of 1.5 °C global warming – Simulation protocol of the Inter-Sectoral Impact Model Intercomparison Project (ISIMIP2b). *Geosci. Model Dev.* **10**, 4321–4345 (2017).

128. S. Siebert, M. Kummu, M. Porkka, P. Döll, N. Ramankutty, B. R. Scanlon, A global data set of the extent of irrigated land from 1900 to 2005. *Hydrol. Earth Syst. Sci.* **19**, 1521–1545 (2015).
129. Y. Wada, M. F. P. Bierkens, Sustainability of global water use: Past reconstruction and future projections. *Environ. Res. Lett.* **9**, 104003 (2014).
130. C. Zarfl, A. E. Lumsdon, J. Berlekamp, L. Tydecks, K. Tockner, A global boom in hydropower dam construction. *Aquat. Sci.* **77**, 161–170 (2015).
131. R. J. Keenan, G. A. Reams, F. Achard, J. V. de Freitas, A. Grainger, E. Lindquist, Dynamics of global forest area: Results from the FAO Global Forest Resources Assessment 2015. *For. Ecol. Manag.* **352**, 9–20 (2015).
132. A. Barnosky, E. Hadly, J. Bascompte, E. L. Berlow, J. H. Brown, M. Fortelius, W. M. Getz, J. Harte, A. Hastings, P. A. Marquet, N. D. Martinez, A. Mooers, P. Roopnarine, G. Vermij, J. W. Williams, R. Gillespie, J. Kitzes, C. Marshall, N. Matzke, D. P. Mindell, E. Revilla, A. B. Smith, Approaching a state shift in Earth's biosphere. *Nature* **486**, 52–58 (2012).
133. H. J. Fowler, G. Lenderink, A. F. Prein, S. Westra, R. P. Allan, N. Ban, R. Barbero, P. Berg, S. Blenkinsop, H. X. Do, S. Guerreiro, J. O. Haerter, E. J. Kendon, E. Lewis, C. Schaer, A. Sharma, G. Villarini, C. Wasko, X. Zhang, Anthropogenic intensification of short-duration rainfall extremes. *Nat. Rev. Earth Environ.* **2**, 107–122 (2021).
134. L. Gudmundsson, J. Boulange, H. X. Do, S. N. Gosling, M. G. Grillakis, A. G. Koutroulis, M. Leonard, J. Liu, N. M. Schmied, L. Papadimitriou, Y. Pokhrel, S. I. Seneviratne, Y. Satoh, W. Thiery, S. Westra, X. Zhang, F. Zhao, Globally observed trends in mean and extreme river flow attributed to climate change. *Science* **371**, 1159–1162 (2021).
135. J. Spinoni, G. Naumann, H. Carrao, P. Barbosa, J. Vogt, World drought frequency, duration, and severity for 1951–2010. *Int. J. Climatol.* **34**, 2792–2804 (2014).
136. T. G. Huntington, Evidence for intensification of the global water cycle: Review and synthesis. *J. Hydrol.* **319**, 83–95 (2006).
137. J. Jägermeyr, A. Pastor, H. Biemans, D. Gerten, Reconciling irrigated food production with environmental flows for sustainable development goals implementation. *Nat. Commun.* **8**, 15900 (2017).
138. A. V. Pastor, F. Ludwig, H. Biemans, H. Hoff, P. Kabat, Accounting for environmental flow requirements in global water assessments. *Hydrol. Earth Syst. Sci.* **18**, 5041–5059 (2014).
139. V. Virkki, E. Alanärä, M. Porkka, L. Ahopelto, T. Gleeson, C. Mohan, L. Wang-Erlandsson, M. Flörke, D. Gerten, S. N. Gosling, N. Hanasaki, H. Müller Schmied, N. Wanders, M. Kummu, Globally widespread and increasing violations of environmental flow envelopes. *Hydrol. Earth Syst. Sci.* **26**, 3315–3336 (2022).
140. P. Greve, B. Orlowsky, B. Mueller, J. Sheffield, M. Reichstein, S. I. Seneviratne, Global assessment of trends in wetting and drying over land. *Nat. Geosci.* **7**, 716–721 (2014).
141. P. Micklin, The aral sea disaster. *Annu. Rev. Earth Planet. Sci.* **35**, 47–72 (2018).
142. W. M. Hammond, A. P. Williams, J. T. Abatzoglou, H. D. Adams, T. Klein, R. López, C. Sáenz-Romero, H. Hartmann, D. D. Breshears, C. D. Allen, Global field observations of tree die-off reveal hotter-drought fingerprint for Earth's forests. *Nat. Commun.* **13**, 1761 (2022).
143. R. S. Cottrell, K. L. Nash, B. S. Halpern, T. A. Remenyi, S. P. Corney, A. Fleming, E. A. Fulton, S. Hornborg, A. Johne, R. A. Watson, J. L. Blanchard, Food production shocks across land and sea. *Nat. Sustain.* **2**, 130–137 (2019).
144. J. Schöngart, F. Wittmann, A. Faria de Resende, C. Assahira, G. de Sousa Lobo, J. R. D. Neves, M. da Rocha, G. B. Mori, A. C. Quaresma, L. O. Demarchi, B. W. Albuquerque, Y. O. Feitosa, G. da Silva Costa, G. V. Feitoza, F. M. Durgante, A. Lopes, S. E. Trumbore, T. S. F. Silva, H. ter Steege, A. L. Val, W. J. Junk, M. T. F. Piedade, The shadow of the Balbina dam: A synthesis of over 35 years of downstream impacts on floodplain forests in Central Amazonia. *Aquat. Conserv. Mar. Freshw. Ecosyst.* **31**, 1117–1135 (2021).
145. B. R. Deemer, J. A. Harrison, S. Li, J. J. Beaulieu, T. DelSontro, N. Barros, J. F. Bezerra-Neto, S. M. Powers, M. A. dos Santos, J. A. Vonk, Greenhouse gas emissions from reservoir water surfaces: A new global synthesis. *BioScience* **66**, 949–964 (2016).
146. A. Clarke, V. Kapustin, Hemispheric aerosol vertical profiles: Anthropogenic impacts on optical depth and cloud nuclei. *Science* **329**, 1488–1492 (2010).
147. P.-A. Monerie, L. J. Wilcox, A. G. Turner, Effects of anthropogenic aerosol and greenhouse gas emissions on northern hemisphere monsoon precipitation: Mechanisms and uncertainty. *J. Clim.* **35**, 2305–2326 (2022).
148. J. Cao, H. Wang, B. Wang, H. Zhao, C. Wang, X. Zhu, Higher sensitivity of northern hemisphere monsoon to anthropogenic aerosol than greenhouse gases. *Geophys. Res. Lett.* **49**, e2022GL100270 (2022).
149. B. Zhuang, Y. Gao, Y. Hu, H. Chen, T. Wang, S. Li, M. Li, M. Xie, Interaction between different mixing aerosol direct effects and East Asian summer monsoon. *Clim. Dyn.* **61**, 1157–1176 (2022).
150. D. M. Westervelt, Y. You, X. Li, M. Ting, D. E. Lee, Y. Ming, Relative importance of greenhouse gases, sulfate, organic carbon, and black carbon aerosol for south asian monsoon rainfall changes. *Geophys. Res. Lett.* **47**, e2020GL088363 (2020).
151. E. D. Galbraith, E. Y. Kwon, A. Gnanadesikan, K. B. Rodgers, S. M. Griffies, D. Bianchi, J. L. Sarmiento, J. P. Dunne, J. Simeon, R. D. Slater, A. T. Wittenberg, I. M. Held, Climate variability and radiocarbon in the CM2Mc Earth system model. *J. Clim.* **24**, 4230–4254 (2011).
152. W. von Bloh, S. Schaphoff, C. Müller, S. Rolinski, K. Waha, S. Zaehle, Implementing the nitrogen cycle into the dynamic global vegetation, hydrology, and crop growth model LPJmL (version 5.0). *Geosci. Model Dev.* **11**, 2789–2812 (2018).
153. P. C. D. Milly, A. B. Shmakin, Global modeling of land water and energy balances. Part I: The land dynamics (LaD) model. *J. Hydrometeorol.* **3**, 283–299 (2002).
154. J. L. Anderson, V. Balaji, A. J. Broccoli, W. F. Cooke, T. L. Delworth, K. W. Dixon, L. J. Donner, K. A. Dunne, S. M. Freidenreich, S. T. Garner, R. G. Gudgel, C. T. Gordon, I. M. Held, R. S. Hemler, L. W. Horowitz, S. A. Klein, T. R. Knutson, P. J. Kushner, A. R. Langenhost, N. C. Lau, Z. Liang, S. L. Malyshev, P. C. D. Milly, M. J. Nath, J. J. Ploshay, V. Ramaswamy, M. D. Schwarzkopf, E. Shevliakova, J. J. Sirutis, B. J. Soden, W. F. Stern, L. A. Thompson, R. J. Wilson, A. T. Wittenberg, B. L. Wyman, The new GFDL global atmosphere and land model AM2-LM2: Evaluationvwith prescribed SST simulations. *J. Clim.* **17**, 4641–4673 (2004).
155. S. Sitch, B. Smith, I. C. Prentice, A. Arneth, A. Bondeau, W. Cramer, J. O. Kaplan, S. Levis, W. Lucht, M. T. Sykes, K. Thonicke, S. Venevsky, Evaluation of ecosystem dynamics, plant geography and terrestrial carbon cycling in the LPJ dynamic global vegetation model. *Glob. Change Biol.* **9**, 161–185 (2003).
156. D. Gerten, S. Schaphoff, U. Haberlandt, W. Lucht, S. Sitch, Terrestrial vegetation and large-scale water balance. Hydrological evaluation of a dynamic global vegetation model. *J. Hydrol.* **286**, 249–270 (2004).
157. A. Bondeau, P. Smith, S. Zaehle, S. Schaphoff, W. Lucht, W. Cramer, D. Gerten, H. Lotze-Campen, C. Müller, M. Reichstein, B. Smith, Modelling the role of agriculture for the 20th century global terrestrial carbon balance. *Glob. Change Biol.* **13**, 1–28 (2007).
158. K. Thonicke, A. Spessa, I. C. Prentice, S. P. Harrison, L. Dong, C. Carmona-Moreno, The influence of vegetation, fire spread and fire behaviour on biomass burning and trace gas emissions: Results from a process-based model. *Biogeosci.* **7**, 1991–2011 (2010).
159. M. Drüke, M. Forkel, W. von Bloh, B. Sakschewski, M. Cardoso, M. Bustamante, J. Kurths, K. Thonicke, Improving the LPJmL4-SPITFIRE vegetation-fire model for South America using satellite data. *Geosci. Model. Dev.* **12**, 5029–2054 (2019).
160. M. Forkel, N. Carvalhais, S. Schaphoff, W. von Bloh, M. Migliavacca, M. Thurner, K. Thonicke, Identifying environmental controls on vegetation greeness phenology through model-data integration. *Biogeosci.* **11**, 7025–7050 (2014).
161. M. Forkel, M. Drüke, M. Thurner, W. Dorigo, S. Schaphoff, K. Thonicke, W. von Bloh, N. Carvalhais, Constraining modelled global vegetation dynamics and carbon turnover using multiple satellite observations. *Sci. Rep.* **9**, 18757 (2019).
162. S. Fader, C. Rost, A. Müller, D. Bondeau, Gerten, virtual water content of temperate cereals and maize: Present and potential future patterns. *J. Hydrol.* **384**, 218–231 (2010).
163. V. Kattsov, R. Federation, C. Reason, S. Africa, A. A. Uk, T. A. Uk, J. Baehr, A. B. Uk, J. Catto, J. S. Canada, A. S. Uk, *Evaluation of climate models (AR5), Climate Change 2013 - The Physical Science Basis* (Cambridge University Press, 2013), pp. 741–866.
164. M. Santoro, O. Cartus, S. Mermoz, A. Bouvet, T. Le Toan, N. Carvalhais, D. Rozendaal, M. Herold, V. Avitabile, S. Quegan, J. Carreiras, Y. Rauste, H. Balzter, C. C. Schmullius, F. M. Seifert, A detailed portrait of the forest aboveground biomass pool for the year 2010 obtained from multiple remote sensing observations. *Geophys. Res. Abstr.* 20, EGU2018-18932 (2018). https://meetingorganizer.copernicus.org/EGU2018/EGU2018-18932.pdf
165. P. Gkatsopoulos, A methodology for calculating cooling from vegetation evapotranspiration for use in urban space microclimate simulations. *Proc. Environ. Sci.* **38**, 477–484 (2017).
166. N. Unger, Human land-use-driven reduction of forest volatiles cools global climate. *Nat. Clim. Change* **4**, 907–910 (2014).
167. W. A. Hoffmann, R. B. Jackson, Vegetation-climate feedbacks in the conversion of tropical savanna to grassland. *J. Clim.* **13**, 1593–1602 (2000).

Acknowledgments: This paper is dedicated to our friend, colleague, and co-author, W.S., who passed away. He was deeply involved in developing this paper. Few have made a greater contribution to describing a pathway for humanity's development in the Anthropocene than W.S. We are grateful for support from K. Noone (aerosols), B. Sakschewski (POEM), and M. Martin (comments). J. Lokrantz (Azote) and D. Biermann (PIK) produced the figures. **Funding:** This work was supported by the European Research Council (Project Earth Resilience in the Anthropocene, ERC-2016-ADG 743080); European Research Council (ERC) under the European

Union's Horizon 2020 research and innovation programme (grant no. 819202); German Federal Ministry for Education and Research (BMBF) through the "PIK Change" framework (grant no. 01LS2001A), and Carlsberg Foundation (Queen Margrethe's and Vigdís Finnbogadóttir´s Interdisciplinary Research Centre on Ocean, Climate, and Society, CF20-0071). POEM development and application were supported by the Volkswagen Foundation (POEM-PBSim—A Simulator for Earth's planetary boundaries, AZ 98046) and work on the biosphere functional integrity boundary by the Global Challenges Foundation. **Author contributions:** K.R., W.S., J.R., and W.L. led the study by conceiving and coordinating the analyses. K.R. led the writing process. J.B., S.E.C., J.F.D., M.D., and I.F. (alphabetical order) collected and collated data, synthesized literature, supported the analyses, prepared the tables and figures, and provided logistical support. The remaining authors (alphabetical order) contributed to the POEM modeling and/or to new analysis of individual boundaries: G.B. (aerosols), W.v.B. (POEM), G.F. (POEM), S.F. (aerosols), D.G. (fresh water), T.G. (fresh water), M.H. (POEM), W.H. (POEM), M.K. (fresh water), C.M. (fresh water), D.N.-B. (biosphere integrity), S.P. (POEM), M.P. (fresh water), S.R. (POEM), S.S. (POEM and functional biosphere integrity), A.T. (land system change), K.T. (POEM), V.V. (fresh water), L.W.-E. (fresh water), and L.W. (aerosols). **Competing interests:** The authors declare that they have no competing interests. **Data and materials availability:** All data needed to evaluate the conclusions in the paper are present in the paper and/or the Supplementary Materials. In addition, the POEM modelling data can be found at https://doi.org/10.5281/zenodo.8032156.

Submitted 19 February 2023
Accepted 12 July 2023
Published 13 September 2023
10.1126/sciadv.adh2458